Tree Physiology 43, 611–629
https://doi.org/10.1093/treephys/tpac137

Research paper

Diplodia sapinea infection reprograms foliar traits of its pine (*Pinus sylvestris* L.) host to death

Bin Hu[1,2,9,†], Zhenshan Liu[1,†], Robert Haensch[1,3], Axel Mithöfer[4], Franziska S. Peters[5], Barbara Vornam[6], Maxim Messerer[7], Klaus Mayer[7], Nicolaus von Wirén[8] and Heinz Rennenberg[1,2]

[1]Center of Molecular Ecophysiology (CMEP), College of Resources and Environment, Southwest University No. 2, Tiansheng Road, Beibei District, 400715 Chongqing, P.R. China; [2]Institute of Forest Sciences, Chair of Tree Physiology, Albert-Ludwigs-Universität Freiburg, Georges-Koehler-Allee 53/54, D-79110 Freiburg, Germany; [3]Institute for Plant Biology, Technische Universität Braunschweig, Humboldtstraße 1, D-38106 Braunschweig, Germany; [4]Research Group Plant Defense Physiology, Max Planck Institute for Chemical Ecology, Hans-Knöll-Straße 8, D-07745 Jena, Germany; [5]Department of Forest Protection, FVA Forest Research Institute of Baden-Württemberg (FVA-BW), Wonnhalde Straße 04, D-79100 Freiburg, Germany; [6]Buesgen Institute Forest Genetics and Forest Tree Breeding, Faculty for Forest Sciences and Forest Ecology, University of Goettingen, Buesgenweg 2, 37077 Goettingen, Germany; [7]Plant Genome and Systems Biology, Helmholtz Center Munich-German Research Center for Environmental Health, 85764 Neuherberg, Germany; [8]Molecular Plant Nutrition, Leibniz-Institute for Plant Genetics and Crop Plant Research (IPK), D-06466 Gatersleben, Germany; [9]Corresponding author (hubjoe@126.com)

Received May 10, 2022; accepted December 4, 2022; handling Editor Pierluigi Bonello

Infection with the necrotrophic fungus *Diplodia sapinea* (Fr.) Fuckel is among the economically and ecologically most devastating diseases of conifers in the northern hemisphere and is accelerated by global climate change. This study aims to characterize the changes mediated by *D. sapinea* infection on its pine host (*Pinus sylvestris* L.) that lead to the death of its needles. For this purpose, we performed an indoor infection experiment and inoculated shoot tips of pine seedlings with virulent *D. sapinea*. The consequences for foliar traits, including the phytohormone profile, were characterized at both the metabolite and transcriptome level. Our results showed that *D. sapinea* infection strongly affected foliar levels of most phytohormones and impaired a multitude of other metabolic and structural foliar traits, such as reactive oxygen species scavenging. Transcriptome analysis revealed that these changes are partially mediated via modified gene expression by fungal exposure. *Diplodia sapinea* appears to overcome the defense reactions of its pine host by reprogramming gene expression and post-transcriptional controls that determine essential foliar metabolic traits such as the phytohormone profile, cell wall composition and antioxidative system.

Keywords: anti-oxidative metabolism, cellulose, chlorophyll, *Diplodia sapinea* infection, lignin, phytohormone profile, ROS accumulation, transcriptome.

Introduction

The ascomycete fungus *Diplodia sapinea* (Fr.) Fuckel (= *Sphaeropsis sapinea* (Fr.) Dyko & B. Sutton, *Diplodia pinea* (Desm.) J. Kickx f.) is reported as one of the most widespread necrotrophic phytopathogens (Fabre et al. 2011). It induces significant dieback disease damages (Diplodia tip blight) on dominant *Pinus* species, particularly on Scots pine (*Pinus sylvestris* L.), in forest ecosystems (Paez and Smith 2018, Brodde et al. 2019). Since this species constitutes one of the most widely distributed conifers in both boreal and temperate ecosystems across European, North American and Asian countries with high ecological and economic values (Luchi et al. 2014), pine forests in these regions suffer large-scale losses due to Diplodia tip blight infection (Stanosz et al. 2001). Prognosticated global climate changes, such as prolonged periods of drought and heat, are supposed to render these conifer forests more vulnerable to *D. sapinea* attacks and to increase the devastation of pine forests by Diplodia tip blight disease in future (Brodde et al. 2019).

Diplodia sapinea is an opportunistic pathogen with a latent endophytic stage (Burgess et al. 2004, Flowers et al. 2006,

[†]These authors contributed equally to this work.

CABI 2019). The fungus can switch its lifestyle from the endophytic (unharmful) to the pathogenic (harmful) state, once this balance is disturbed by stress-inducing environmental conditions that weaken its host, such as hail, heat and drought (Stanosz et al. 2001, Bußkamp 2018, Blumenstein et al. 2021, Oliva et al. 2021). However, the mechanisms of interaction between the latent *D. sapinea* pathogen and its host Scots pine are still poorly understood (e.g., Terhonen et al. 2019, Hu et al. 2021).

The vital defense responses of plant to fungal pathogens include programmed cell death (PCD) (also recognized as hypersensitive response (HR)), lignification for reinforcement of cell walls, trigging the plant antioxidative system and the hormonal signaling network (Pieterse et al. 2009, Torres 2010, Spoel and Dong 2012, Rojas et al. 2014). Thus, infection of necrotrophic pathogens such as *D. sapinea* often result in changes of primary and secondary metabolism, tissue dieback, nutrient resorption from host living tissue cells for fungal invasion, and xylem and/or phloem destruction of their host plants (Berger et al. 2007). In addition, necrotrophic pathogens also affect the water balance of host plant by mediating its stomatal closure, concomitant with a further reduction of photosynthetic carbon-fixation (Oliva et al. 2014).

Phytohormones constitute cellular signaling molecules with vital roles in regulation of plant responses to pathogen infection (Vanstraelen and Benkova 2012). Particularly, both salicylic acid (SA)- and jasmonic acid (JA)-mediated signaling pathways are considered as backbones of plant responses to pathogen invasion (Pieterse et al. 2012). For tree species, relevant knowledge is obtained mostly through exogenous hormone application, whereas information on how indigenous JA and SA signaling of diseased host plants responds to pathogen invasion still needs to be elucidated (Gould et al. 2009). Such in-planta analysis is essential to characterize the antagonistic and (or) synergistic regulatory interactions among phytohormonal signal pathways in plant defense responses, i.e., the phytohormone crosstalk. However, such information is scarce for woody host plants (Hu et al. 2017, 2018, 2021). Intending to develop a model system for Diplodia–pine interactions, we conducted an inoculation experiment with 4-year-old pine saplings in the greenhouse. The results showed that *D. sapinea* induced systemic responses in its host that caused subsequent destruction of non-infected needles but prevented damage to the roots (Hu et al. 2021). However, it remains unknown if these systemic responses differ from the direct responses at both the metabolic and molecular level in foliar tissues infected by *D. sapinea*.

In this context, we intended to elucidate the direct molecular and metabolic responses of foliar tissues to infection by *D. sapinea* and compare these responses with systemic defense reactions previously reported (Hu et al. 2021). For this purpose, we infected pine saplings with isolated *D. sapinea* strain on the tips and compared the molecular and metabolic responses of symptomatic needles with non-infected saplings. We hypothesize that pine shoot tips infected with *D. sapinea* will show (i) significant changes in the stress-related phytohormone profile, (ii) metabolic changes similar to drought stress, and (iii) specific defense reactions such as changes in ROS contents and cell wall composition that (iv) are mainly controlled at the transcriptional level.

Materials and methods

Plant materials preparation

Scots pine saplings (*Pinus sylvestris* L.) of the provenance '85104', originating from the German central and eastern lowland, were purchased from a commercial tree nursery (G.J. Steingaesser & Comp. GmbH, Miltenberg, Germany) at a mean height of 95 ± 3 cm. Plants were 4 years old and grown in square pots (18 × 18 × 25 cm) filled with commercial potting soil (Corthum; Corthum Breisgau GmbH, Herbolzheim, Germany) in a greenhouse (47° 58' 26.724" N, 7° 50' 36.06" E) for 4–6 weeks from early June to July, 2016 before infection with *D. sapinea*. All pine saplings were watered four times a week to ensure sufficient water supply and fertilized once with a 1% solution of Universol Water Soluble Fertilizer Blue (18-11-18 N:P:K + 2·5% MgO + TE; Everris, Ipswich, UK). During the growing period, the ambient air mean temperature and relative humidity were 28.2 ± 2.5 °C/22.3 ± 2.2 °C and 55.5 ± 8.7%/54.3 ± 6.7% (16 h and 8 h, day and night), respectively, as described by Hu et al. (2021).

Experimental design and pathogen infection

Two treatments were established, i.e., saplings sprayed with *D. sapinea*-free malt-peptone broth (non-infected control) and saplings infected by spraying malt-peptone broth containing *D. sapinea* (infected) (Hu et al. 2021). Pine seedlings of the same height and diameter range were selected for the infection experiment (Vornam et al. 2019). The replicates included six pine saplings per treatment ($n = 6$). The *D. sapinea* strain used in this study was isolated from symptomatic tissues of Scots pine tips in northeastern German forests representing pathogenic strains and stored in the Northwest German Forest Research Institute (NW-FVA) strain collection according to Bußkamp et al. (2020). The origin of the strain is described in detail by Blumenstein et al. (2020). The strain of *D. sapinea* used in this study was initially identified by the mycelial morphotypes and further characterized based on micro-morphological characters and DNA sequence analysis as described in Bußkamp et al. (2020). For this purpose, the selected strain was stored on slants with malt yeast peptone (MYP) agar at 4 °C (Langer 1994). From the selected morphotype, 1–2 mg tissue was suspended in 100 μl TE buffer in a 1.5-ml tube. A microwave (600 W) was used twice for 1 min each time, with a pause of 30 s, to break up cells. Tubes were cooled to −20 °C for 20 min and centrifuged at 10,000*g* for

5 min. A 100 times diluted portion of the supernatant was used for DNA analysis by the polymerase chain reaction (PCR). Primer pairs for amplification of the ITS1, 5.8S and ITS2 regions were ITS1F/ITS4 or ITS1/ITS4 (White et al. 1990, Gardes and Bruns 1993). PCR was performed with 45 μl Master mix (QIAGEN, Hilden, Germany) and 5 μl of extracted DNA. PCR was carried out with initial denaturation at 94 °C for 3 min, followed by 29 cycles of denaturation at 94 °C for 30 s, annealing at 55 °C for 45 s and extension at 72 °C for 60 s; final elongation was performed at 72 °C for 7 min. PCR products were separated on 1% agarose gel stained with GelRed fluorescence dye (Biotium, Hayward, CA, USA), followed by cleaning with the QIAquick PCR Purification kit (QIAGEN, Hilden, Germany). Sanger sequencing of purified products (Sanger et al. 1977) was commissioned at GATC Biotech (Cologne, Germany). Editing and alignment of DNA sequences were performed with MEGA6 (Tamura et al. 2013) and, thereafter, sequences were submitted to GenBank (accession No. MG098333).

Prior to inoculation, fungal isolates were plated on a malt-peptone broth (3% malt, 0.5% peptone) and grown at 25 °C for 1 week as described by Schumacher (2012). Subsequently, 20 ml of inoculated malt-peptone broth was added into 500-ml fresh Malt Extract Broth and incubated for 1 week at 25 °C to obtain a mycelial solution (Vornam et al. 2019). The mycelial solution was homogenized (UltraTurrax®, IKA, Staufen, Germany) and diluted at a ratio of 1:2 with fresh malt-peptone broth to obtain the fungal suspension used for inoculation (Hu et al. 2021). The *D. sapinea* infection was conducted on 16 July 2016. Needles of current and previous year shoots of six selected pine saplings were individually sprayed with fungal suspension for ca 3 s with a sprayer bottle. Another set of six control (non-infected) Scots pine saplings, sprayed with broth without fungal mycelium, was used as non-infected control (details as described by Vornam et al. 2019). The infected and non-infected saplings were placed separately in two closed transparent UV-foil greenhouses set up in close vicinity under similar environmental conditions. After infection, the infected pine saplings were moved and kept under enhanced humidity for 3 days in a smaller greenhouse to enforce the virulence of the fungal mycelium. Thereafter, the saplings were moved back to the former foil greenhouse (Vornam et al. 2019). Disease development and severity of infection were assessed from the morning of the third day (21 July 2016) after *D. sapinea* infection. The occurrence of brown current-year needles indicated that the infection was successful.

As *D. sapinea* can infect pines without causing symptoms in its endophytic stage, we chose three plants per treatment ($n = 3$) randomly and examined the shoots and needles before the inoculation experiment for possible colonization by *D. sapinea*. After the termination of experiment, three pine plants per treatment ($n = 3$) were also selected to test the presence and/or absence of *D. sapinea*. For these purposes, the selected pine shoot tips were surface-sterilized (1 min in 70% EtOH/5 min 4% NaOCl/1 min 70% EtOH) and cut into pieces (0.5 cm). The pieces were plated on Petri dishes with MYP agar (Langer 1994). In addition, three shoot segments were placed on MYP medium in a 90-mm-diameter plastic Petri dish and incubated for up to 3 weeks at room temperature (ca 22 °C) and ambient daylight. Shoot segments on dishes were visually checked every week for developing colonies of *D. sapinea* and other outgrowing fungi. Emerging mycelia were sub-cultured separately on MYP medium. Subsequently, the isolated fungal strains were stored on MYP slants at 4 °C, first identified by morphology, followed by DNA extraction and ITS region sequencing to confirm identity by the procedures described above (Bußkamp et al. 2020). The sequences obtained were aligned with BLASTN (Zhang et al. 2000) to test if the isolate was the same as used for the experimental infection. The results showed that before infection, no endophytic *D. sapinea* was present in the pine plants. In addition, at the end of the infection experiment, *D. sapinea* could only be isolated from sprayed shoot sections of the infected plants. The isolated strain was the same as the initial *D. sapinea* strain used for infection.

Plant sample harvest

Harvest of needle samples was started in the morning of the seventh day after infection (25 July). At this time, the infected current- and previous-year needles on pine shoot tips already showed the dominant brown color of necrotic tissues, whereas non-inoculated needles located basipetal on the same stem did not show visible symptom of infection (the symptom details of needles are shown in Figure 1 (and Figure S1 available as Supplementary data) of Hu et al. 2021). From the six pine plants each of the infection and control treatments, 5–7 g fresh weight (FW) of symptomatic (dominant brown color of infected current- and previous-year needles of infected plants) and asymptomatic needles (without visible symptom of needles of non-infected control plants) were collected at similar distance from previous year branches with a scissor for biochemical analyses. Additional needle samples (ca 3–5 g FW) of infected and control plants were collected in the same places for transcriptomic analysis. All harvested needle samples were immediately shock-frozen in liquid N_2, and stored at −80 °C (Hu et al. 2021). The needle samples for biochemical analysis were homogenized to a fine powder in liquid N_2.

Biochemical analyses

Phytohormone quantification by LC–MS/MS Phytohormone analyses were carried out with homogenized needle samples lyophilized for 5 days (Alpha 2–4 with an LDC-1 M module for system control; Martin Christ, Germany). For JA, hydroxy-JA (OH-JA), jasmonoyl-L-isoleucine (JA-Ile), hydroxy-JA-Ile (OH-JA-Ile), carboxy-JA-Ile (COOH-JA-Ile), 12-oxo-phytodienoic acid (*cis*-OPDA), SA, abscisic acid (ABA), indole-3-acetic acid (IAA) and cytokinin (CKs) determination, aliquots of 25 mg lyophilized tissue samples were extracted and analyzed as

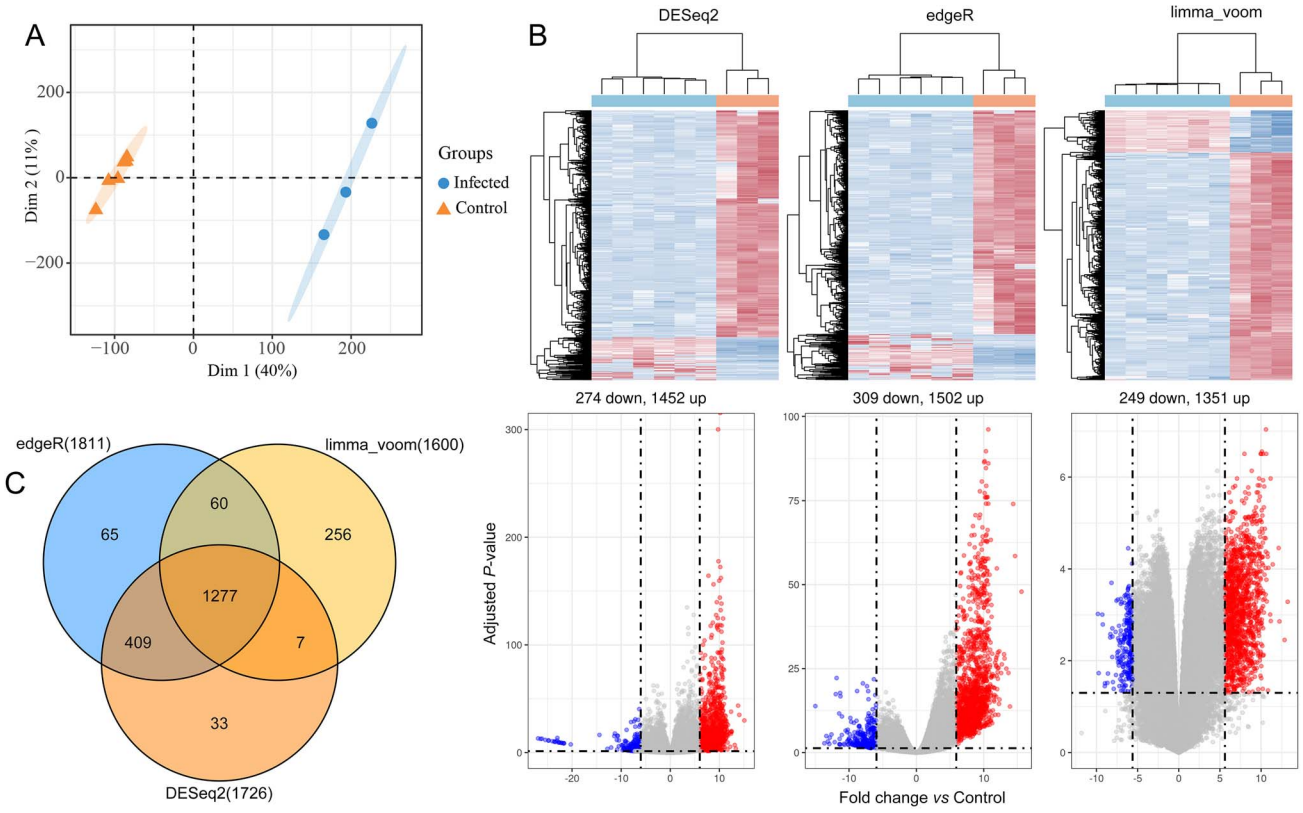

Figure 1. Identification of DEGs between non-infected controls and infected needles. (A) PLS-DA plots of transcripts identified by RNA-seq of pine needles infected by *Diplodia sapinea* at 7 days post-infection. The first (Dim 1) and second (Dim 2) principal components explain 51% of the variance. (B) DEGs identified by three methods, edgeR, limma(voom) and DESeq2. (C) Venn diagram of DEGs identified by these three methods.

described by Vadassery et al. (2012) with minor modifications. Phytohormone separation and quantification were performed by high-performance liquid chromatography coupled to tandem mass spectrometry (HPLC–MS/MS) (Agilent 1260, Agilent Technologies, Santa Clara, CA, USA; API 5000, Applied Biosystems, Darmstadt, Germany) with a Zorbax Eclipse XDB-C18 column (50 × 4.6 mm, 1.8 μm; Agilent Technologies, Santa Clara, CA, USA). About 60 ng D4-SA (Santa Cruz Biotechnology, CA, USA), 60 ng D6-JA (HPC Standards GmbH, Borsdorf, Germany), 60 ng D6-ABA (Santa Cruz Biotechnology, CA, USA), 12 ng D6-JA-Ile (HPC Standards GmbH, Borsdorf, Germany) and 60 ng of D5-IAA (OlChemIm s.r.o., Olomouc, Czech Republic) were added to each sample as deuterated internal standards. The detailed MS protocol in negative ionization mode has been described previously by Heyer et al. (2018). Analyst 1.5 software (Applied Biosystems) was used for dataset processing. IAA was quantified with the same LC–MS/MS system as described above applying the same chromatographic conditions, but using the MS in positive ionization mode. The ion-spray voltage was maintained at 5500 eV. The turbo gas temperature was set at 700 °C. Nebulizing gas was set at 70 p.s.i., curtain gas at 30 p.s.i., heating gas at 60 p.s.i. and collision gas at 4 p.s.i.. Multiple reaction monitoring was used for IAA analysis by monitoring analyte parent ion → product ion: m/z 176 → 130 for IAA; m/z 181 → 134 + m/z 181 → 133 for d5-indol-3-acetic acid (internal standard for assay of IAA). Collision energy was 19 V; de-clustering potential was 31 V.

For determination of CKs, aliquots of 50 mg homogenized lyophilized fine needle powder were extracted using methanol/water (1:1, v/v) and purified by solid-phase extraction. CKs were eluted with 1 ml 0.35 M ammonia (NH_3) in 60% MeOH. Dried eluents were re-solved in 50–100 μl 25% MeOH and quantified by liquid chromatography-electrospray ionization-tandem mass spectrometry (LC-ESI-MS/MS) (UPLC-Xevo-TQ-MS, Waters, Eschborn, Germany). MS datasets were processed using TargetLynx V4.1 SCN 904 with internal standard correction. The details of CK extraction, separation and quantification including external and internal standards were described by Eggert and von Wirén (2017). The limit of quantification for CKs was between 0.5 and 250 nM g^{-1} sample dry weight (DW). For each phytohormone species, samples from four replicate pine plants per treatment were analyzed ($n = 4$).

Determination of $\delta^{13}C$ natural abundance and total carbon and nitrogen $\delta^{13}C$ natural abundance and total carbon and nitrogen contents were determined in aliquots of needle powder dried at 60 °C for 48 h. Samples (2.0–2.5 mg) were weighed into tin capsules (IVA Analysentechnik, Meerbusch, Germany)

and analyzed using a carbon/nitrogen elemental analyzer (NA 2500, CE Instruments, Milan, Italy) coupled via a Conflo 2 * ROMAN interface (Finnigan MAT GmbH, Bremen, Germany) to an isotope ratio mass spectrometer (Delta plus, Thermo Finnigan MAT GmbH, Bremen, Germany) as previously described in Geßler et al. (2005). Glutamic acid was used as working standard and calibrated against the primary standard USGS 40 (glutamic acid, $\delta^{13}C_{PDB} = -26.389$, internal standard range between −33.63 and − 11.21‰). For $\delta^{13}C$ determination, working standards were analyzed after every 10th sample to detect any potential instrument drift over time.

Needle pigment analysis Chlorophyll (Chl) *a, b* and carotenoids (Car) were extracted as described by Mantoura et al. (1997). For this purpose, homogenized needle powder (50 mg FW) was mixed with 700 μl 98% methanol containing 0.5 M ammonium acetate (pH 7.1). After 2-h incubation in the dark at 4 °C, the supernatant containing the pigments was separated from the pellet by centrifugation at 15,000*g* for 5 min at 4 °C. The pellet was subsequently re-suspended twice in methanol and subjected again to centrifugation at 15,000*g* for 5 min at 4 °C. Needle pigments were quantified in the combined extracts using a Genesys 10S spectrophotometer (Fisher Scientific, Waltham, MA, USA) at 470.0, 652.4 and 665.2 nm (Lichtenthaler 1987) and expressed as mg g^{-1} DW.

Determination of hydrogen peroxide The concentrations of the reactive oxygen species (ROS) hydrogen peroxide (H_2O_2) were determined according to Velikova et al. (2000). Aliquots of 50 mg FW needle powder were mixed with 1 ml 1% (w v^{-1}) trichloroacetic acid (TCA) on ice. The homogenate was centrifuged at 15,000*g* for 15 min at 4 °C. Subsequently, 250 μl supernatant was added to 250 μl 100 mM phosphate buffer (pH 7.0) and 500 μl 1 M KI. The H_2O_2 content of the supernatant was determined by comparing its absorbance at 390 nm to a standard calibration curve and was expressed as μmol g^{-1} DW.

Determination of structural biomass and preparation for lignin and holo-cellulose analyses Structural biomass (SBM) of needle samples was extracted and quantified as reported by Blaschke et al. (2002). For this purpose, 500 mg dry needle powder was suspended in 50 ml washing buffer (100 mM K_2HPO_4/KH_2PO_4, pH 7.8, 0.5% Triton X-100), slowly stirred for 30 min at room temperature and centrifugated at 5500*g* for 20 min. The pellet was re-suspended in washing buffer and washed again as above. Subsequently, the pellet was washed four times (30 min each time) with 100% methanol (MeOH). The resulting pellet consisted mainly of cell wall material and was defined as SBM. To get rid of esterified phenolic compounds, which interfere with lignin determination, especially in needles of pine saplings, the pellet was subjected to alkaline hydrolysis under N_2 (2 M NaOH for 1 h). The hydrolyzed pellet was washed twice with distilled water, dried at 80 °C for 12 h, weighed and used for further gravimetric lignin and holo-cellulose (cellulose and hemicellulose) determination (Brinkmann et al. 2002).

Lignin and holo-cellulose analysis For the determination of lignin in pine needle samples (modified after Van Soest 1963, Rowland and Roberts 1994), dried hydrolyzed SBM pellets of needle tissue were weighed (W1) into 250 ml Erlenmeyer flasks with 30 ml 37% hydrochloric acid and 3 ml 97% sulfuric acid. The solution was kept under the fume-hood overnight. Subsequently, the mixture was transferred into a 1000 ml glass beaker, 500 ml distilled water were added and the mixture was boiled for 10 min under continuous stirring. The boiled solution was filtered and the filtrate oven dried (105 °C for 24 h) on a pre-weighed sinter (W2) (Robu-Glas, No. 2, 16–40 μm, Jena, Germany). Subsequently, samples were washed with 500 ml hot distilled water under vacuum until the residue was acid-free (pH 7.0). The filtrate was dried again on the sinter at 105 °C for 24 h, cooled and weighed (W3) to determine the DW of the residue. Lignin contents (% of SBM) were calculated as follows:

$$\textit{Lignin content}\ (\%SBM) = \frac{(W3 - W2) \times 100}{W1}$$

The holo-cellulose (cellulose and hemicellulose) content of SBM (%) was calculated by subtracting the lignin content (%) from total hydrolyzed SBM.

Determination of glutathione reductase and dehydroascorbate reductase enzyme activities For determination of glutathione reductase (GR) and dehydroascorbate reductase (DHAR) in vitro enzyme activities, aliquots of 50 mg homogenized frozen needle were extracted for 10 min on ice in 1.5 ml pre-cooled potassium phosphate (KPP) extraction buffer (100 mM K_2HPO_4/KH_2PO_4, pH 7.8, 1% Triton X-100) containing 80 mg pre-washed polyvinylpolypyrrolidone (PVPP 6755, Sigma-Aldrich Inc., Steinheim, Germany). After centrifugation (15 min, 15,000*g* at 4 °C), the supernatant was passed through a Sephadex column (NAP 5, GE Healthcare), as described by Arab et al. (2016). The fresh extracts were immediately used for kinetic analyses with a UV-DU650 spectrophotometer (Beckman Coulter Inc., Fullerton, CA, USA) at 340 and 265 nm for GR and DHAR activity, respectively. The activity of GR was determined by monitoring glutathione dependent oxidation of 1.25 mM NADPH at 340 nm as described by Polle et al. (1990). DHAR activity was assayed directly by following the increase in absorbance at 265 nm, resulting from GSH-dependent production of ascorbate. The assay mixture consisted of 8 mM DHA, 10 mM GSH and 100 mM potassium phosphate buffer (pH 6.1). To determine the recovery rates of GR and DHAR, internal standards

(Sigma-Aldrich Chemie GmbH, Steinheim, Germany) were added during extraction. The mean recovery rates amounted to 80.4 ± 5.1% for GR and 91.0 ± 4.6% for DHAR. Measurements were technically performed in triplicate for all samples ($n = 6$).

Extraction and quantification of water-soluble thiols Thiols were extracted and quantified from needle tissue by the modification of the method of Schupp and Rennenberg (1988) previously described by Strohm et al. (1995). Thiols in needle extracts were quantified as monobromobimane derivatives with an ACQUITY UPLC system by fluorescence detection (Waters Corp., Milford MA, USA). Standards were subjected to the same reduction and derivatization procedure. The mean recovery rates of internal GSH standards added to needle extracts were 82.1 ± 1.5%. Measurements were performed in triplicate for each sample ($n = 6$).

Extraction and quantification of ascorbic acid Ascorbic acid contents were determined according to Haberer et al. (2007). Aliquots of 50 mg FW of frozen and homogenized needle powder were extracted in 500 μl 5% meta-H_3PO_4 solution, vortexed and centrifuged for 30 min at 4 °C and 14,000*g*. Two aliquots of 100 μl supernatant, each, were mixed with 20 μl 1.5 M triethanolamine and 100 μl sodium phosphate buffer (150 mM, pH 7.4) in safe seal micro-tubes (2 ml, Sarstedt AG & CO, Nuembrecht, Germany) for each sample, one to determine the amounts of reduced ascorbate, the other to determine the total ascorbate content. Total ascorbate contents were determined after reduction with 50 μl Dithiothreitol (DTT) (10 mM) and incubation at room temperature for 15 min. The excess DTT was removed by adding 50 μl NEM (0.5%). Samples for the determination of both, reduced and total ascorbic acid contents were further processed by adding 200 μl TCA (10%), 200 μl orthophosphoric acid (44%), 200 μl 2.2′–dipyridil (4% in ethanol) and 100 μl $FeCl_3$ (3%). Samples were mixed and incubated at 37 °C for 60 min. Absorption at 525 nm was determined with a UV-DU650 spectrophotometer (Beckman Coulter Inc., Fullerton, CA, USA). L-ascorbic acid (Sigma-Aldrich Chemie GmbH, Steinheim, Germany, 1.5 mg ml^{-1}) was used as a standard. The mean recovery rate of ascorbate internal standards added to needle extracts amounted to 93.5 ± 2.2%.

Dry weight and water content determination Aliquots (~100 mg FW) of homogenized needle material were dried at 60 °C for 48 h to weight constancy for DW determination. Water contents were calculated as the difference between fresh and DW as below:

$$Water\ content\ (mgH_2O/mgDW) = \frac{FW - DW}{DW}$$

All physiological and biochemical parameters determined in the present study were calculated and expressed on a DW basis.

Statistical analyses of biochemical data Statistical tests of results from biochemical analyses were based on needles material from six replicate pine plants ($n = 6$) except for phytohormone analyses ($n = 4$), either infected with *D. sapinea* or used as controls. Data were first tested by either Kolmogorov–Smirnov or Shapiro–Wilk tests for normal distribution. Where necessary, data were transformed using either log- or square-root transformation to satisfy the assumptions of normality and homogeneity of variance. Significant differences between needle samples of *D. sapinea*-infected and non-infected control plants were identified using unpaired *t*-tests. Differences were considered significant at $P < 0.05$. All statistical analyses and graphical work were performed using SPSS 22.0 (SPSS Inc., Chicago, IL, USA) and Sigmaplot 14.0 (Systat Software GmbH, Erkrath, Germany).

To compare biochemical and phytohormone data of needles from *D. sapinea*-infected and non-infected control plants, raw data were log transformed and subjected to partial least squares-discriminant analysis (PLS-DA). Subsequently, PLS-DA loading plots were generated and hierarchical cluster analysis (HCA) was performed for the generation of heat maps. For this purpose, data were processed using the MetaboAnalyst 5.0 software (http://www.metaboanalyst.ca) (Pang et al. 2021).

Transcriptome analysis Total RNA of randomly selected needle samples of three *D. sapinea*-infected pine trees and three control trees were extracted for RNA-sequencing (RNA-Seq) using the RNeasy Plant Mini kit (Qiagen, https://www.qiagen.com) according to the manufacturer's instructions ($n = 3$). RNA concentration and quality were confirmed using a Nanodrop ND-1000 spectrophotometer (ThermoFisher Scientific, Weil am Rhein, Germany) and a 2100 Bioanalyzer (Agilent Technologies). Library preparation and sequencing were performed by the Transcriptome and Genome Analysis Laboratory (TAL, Goettingen, Germany) using the TruSeq RNA mRNA Library Preparation kit v2 and a HiSeq4000 (SR; 1 × 50 bp; 30 Mi reads/sample) (Illumina, Berlin, Germany), respectively. Raw read data quality was verified with fastQC (Andrews 2014), trimmed using Trimmomatic v0.30 (Bolger et al. 2014) to remove low quality reads and reads shorter than 30 nucleotides, and mapped to the genomes of two *D. sapinea* strains CMW 190 and CMW 39103 (Van et al. 2014) via hisat2 (Kim et al. 2015) to filter out fungal sequences.

De novo assembly was carried out using clean reads from all six plant individuals to obtain a transcriptome that was unbiased and representative of both infected and control groups to accurately identify genes that are differentially expressed between treatments. We performed the assembly using the Trinity software package (version 2.12.0) with parameter setting of '-min_kmer_cov2', a fixed k-mer size of 25 and other default parameters (Grabherr et al. 2013). Transcripts not well supported by reads or of high similarity were removed with two filtering steps. First, reads from all samples were individually

mapped back to the assembled transcriptome using RNA-Seq by Expectation-Maximization (RSEM) (Dewey and Li 2011). Transcripts with abundance superior to one Fragments Per Kilobase of transcript per Million mapped reads (FPKM) across all samples were considered for further analysis. To remove highly similar or redundant transcripts, we merged transcripts with higher sequence identity than 95% using CD-HIT-EST (Li and Godzik 2006). The quality of the assembly was evaluated in two ways. First, the completeness of the assembly and the accuracy of gene sets was evaluated using the BUSCO (benchmarking universal single-copy orthologs) software (Simão et al. 2015) against the plant embryophyta_odb10 dataset to determine the proportion of a core-set of 1614 highly conserved eukaryotic genes in transcriptome mode. Second, we mapped the RNA reads to this draft assembly to evaluate the RNA reads mapping rate using kallisto (Bray et al. 2016).

Transcripts per million values were used to estimate gene expression under both treatments. The application of multiple statistical packages to identify a conservative set of genes that were differentially expressed has been recommended as a strategy to minimize false positives in differentially expressed gene (DEG) analysis (Zhang et al. 2014). Therefore, differential expression analysis was performed using three methods. EdgeR (Robinson et al. 2010), limma (voom) (Law et al. 2014) and DESeq2 (Oshlack et al. 2010) were used with more strict criteria to determine candidate DEGs, *i.e.,* any gene with a false discovery rate of < 0.05 and a |log2FoldChange| higher than a cutoff of mean [abs(log2FoldChange)] + 2 × sd[abs(log2FoldChange)]. The BLASTX program was then used to annotate the transcript sequences based on sequence homology against the nr, swissprot, Gene Ontology (GO) and Kyoto Encyclopedia of Genes and Genomes (KEGG) databases with an E-value cut-off of 1×10^{-10}. Gene ontology and KEGG enrichment analysis of the DEGs were performed and visualized with the clusterProfiler R package (Yu et al. 2012). The Benjamini–Hochberg correction was used for multiple tests and an adjusted *P*-value of < 0.05 was considered to be significantly enriched.

Results

Diplodia sapinea infection modifies the transcriptome of infected pine needles

To elucidate to what extent the responses of structural and metabolic traits of pine needles to *D. sapinea* infection are mediated by altered gene expression, genome-wide transcript abundances in pine needles were compared between control and pathogen infection treatments. The Trinity-derived transcriptome assembly contained a total of 55,068 transcripts with an N50 of 1586 bp and an average length of 862 bp. About 88.3% of total reads were mapped back onto this transcriptome. BUSCO score (Table S5 available as Supplementary data at *Tree Physiology* Online) suggested no contamination and good assembly quality. PLS-DA showed that the controls were tightly clustered and clearly separated from pathogen-infected samples (Figure 1A), indicating strong transcriptomic responses to the *D. sapinea* infection.

As expected, edgeR, limma (voom) and DESeq2 identified different sets of DEGs (Figure 1B). Given the relatively stringent cut-off, these analyses collectively yielded 2035 potential DEGs identified by at least one method, constituting ∼3.7% of the expressed genes in the pine host. Functional enrichment analysis revealed that the DEGs between controls and infected samples were mainly enriched for plant defense responses (*i.e.,* response to fungus, chitin, wounding), oxidoreductase activity, ROS scavenging, biosynthesis/regulation of phytohormones and the biosynthesis of specific metabolites, including pinene, oxylipin and flavonoids (Figure 2A; Tables S6 and S7 available as Supplementary data at *Tree Physiology* Online). KEGG pathway enrichment analysis of these DEGs (*q*-value < 0.05) suggested that DEGs were mainly enriched in phytohormone signal transduction, plant–pathogen interaction, transcription factors and several biosynthesis pathways, including those associated with phenylpropanoid, glutathione, amino sugar and nucleotide sugar metabolism (Figure 2; Tables S6 and S7 available as Supplementary data at *Tree Physiology* Online).

Phytohormone biosynthesis is reprogrammed by D. sapinea infection

To identify direct foliar responses induced by virulent *D. sapinea* exposure, we compared the phytohormone profile of infected pine needles with non-infected controls. A total of 22 phytohormones were identified across all plants following infection with *D. sapinea* at 7 days post-infection (Figure 3A). PLS-DA showed a clear separation between the control and *D. sapinea* induced pine phytohormones along the first axis (Figure 3A). Phytohormones like JA and its derivatives with variable importance in projection values ≥1.0 contributed most to this separation. HCA showed the separation pattern accordingly (Figure 3B). Thus, *D. sapinea* infection induces significant phytohormonal changes in the infected pine needles (Figure 3A and B).

Upon *D. sapinea* infection, the levels of most detected foliar phytohormones were strongly upregulated compared with controls (Table S1 available as Supplementary data at *Tree Physiology* Online), *i.e.,* adenine, ABA, SA, JA-Ile as well as total CK and most of its components. In addition, JA, OH-JA, OH-JA-Ile and carboxy-jasmonoyl-L-isoleucine (COOH-JA-Ile) were detected in infected needles, but not in needles of control plants (Table S1 available as Supplementary data at *Tree Physiology* Online). Only IAA contents showed reduced patterns in needles of infected pine saplings compared with control saplings. Adenosine and several CKs contents showed unaffected patterns by *D. sapinea* infection (Table S1 available as Supplementary data at *Tree Physiology* Online).

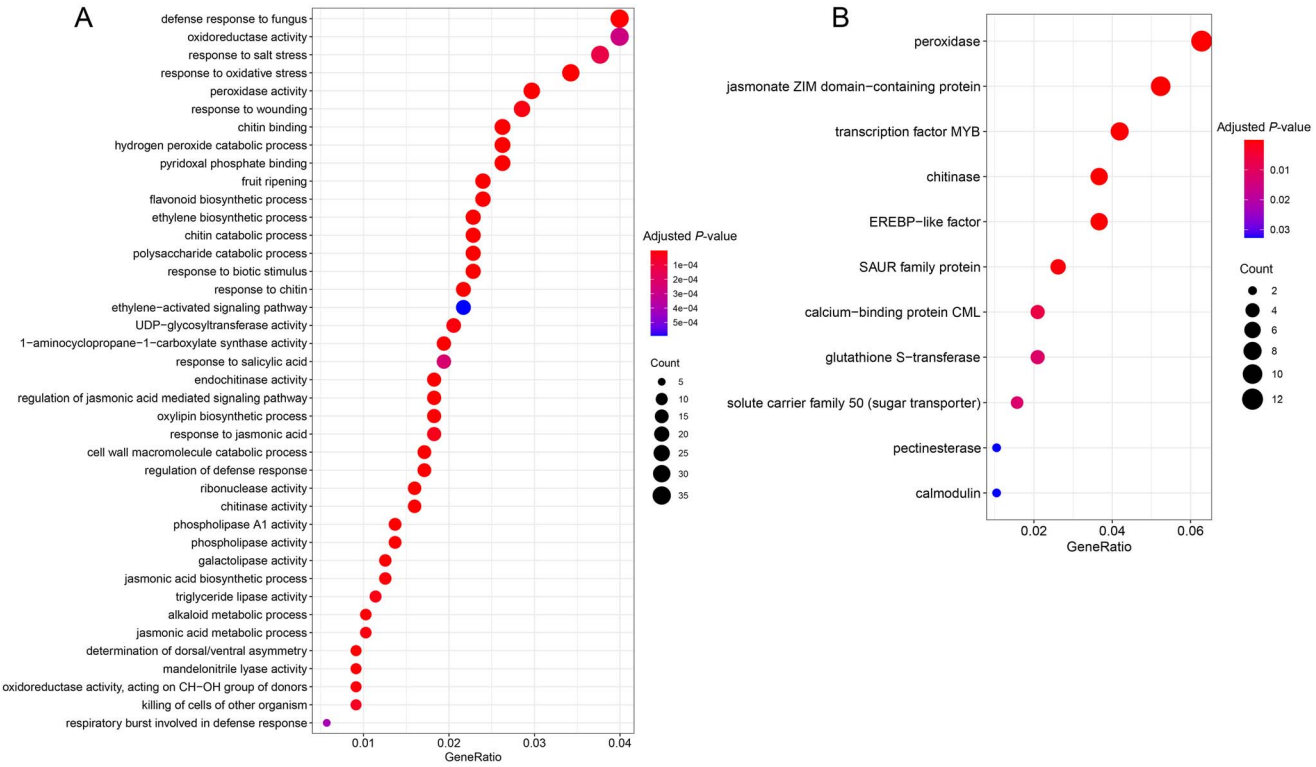

Figure 2. Functional enrichment analysis of DEGs against the databases of (A) GO and (B) KEGG pathways in the pine transcriptome infected by *D. sapinea*.

Transcriptome analysis largely uncovered the molecular mechanism that mediated the significant changes of the phytohormone profile in infected needles (Figure 4). In the pathway of ABA metabolism, however, significantly upregulated key genes not only included phytoene synthase (CrtB), and β-carotene hydroxylase (CrtZ) involved in ABA synthesis, but also abscisate beta-glucosyltransferase (AOG) and ABA 8′-hydroxylases (CYP707A) involved in ABA catabolism. In the downstream ABA-mediated stomatal closure pathway, the expression of *protein phosphatase 2C (PP2C)* and putative sulfate-permeable R-type/quick-activating anion channel1 (*QUAC1*/*ALMT12*) was significantly increased in the *D. sapinea*-infected needles. Different from these balanced changes in ABA metabolism, 12-oxo-phytodienoic acid reductase (*OPR*) in the JA biosynthesis pathway and 1-aminocyclopropane-1-carboxylic synthase (*ACS*) in the ethylene biosynthesis pathway that constitute rate-limiting enzymes of biosynthesis of these phytohormones were both upregulated to ∼1000-fold compared with controls. We also found that the JA-related synthesis enzymes lipoxygenase (*LOX2S*) and OPC-8:CoA ligase 1 (*OPCL1*) were upregulated (Figure 4). Among the four known pathways of Trp-dependent IAA biosynthesis (Mashiguchi et al. 2011), only the pathway through *YUCCA* genes was detected in pine. However, expression pattern of most genes involved in this pathway was not affected by *D. sapinea* infection or even slightly downregulated, despite an enhanced expression of genes of the chorismate precursor. At the same time, the expression of auxin transporter protein 1 (*AUX1*) was significantly induced, indicating that reduced IAA levels may not be a consequence of reduced synthesis, but rather of enhanced export. At the same time, the induction of small auxin upregulated RNA (*SAUR*) genes may indicate the induction of early senescence. In the isochorismate route, both *isochorismate synthases menF* and *PHYLLO* were downregulated, whereas two transcripts of the *ENHANCED PSEUDOMONAS SUSCEPTIBILITY 1 (EPS1)*, an acyltransferase that spontaneously decomposes isochorismate-9-glutamate into SA and 2-hydroxy-acryloyl-N-glutamate, were significantly upregulated upon *D. sapinea* infection. In the phenylalanine route, almost all related genes showed increased expression, particularly for *PAL*, the key enzyme to catalyze the deamination of phenylalanine to trans-cinnamic acid as part of the phenylpropanoid pathway in SA biosynthesis in response to *D. sapinea* infection in pine (Figure 4). We did not observe signaling reactions induced by the CK zeatin at the transcriptomic level.

General structural and metabolic responses of pine needles to the infection with D. sapinea To detect metabolic differences between *D. sapinea*-infected needles and control plants, tissue hydration, SBM, cell wall and pigment composition, $\delta^{13}C$ natural abundance, foliar total nitrogen and carbon contents, antioxidant

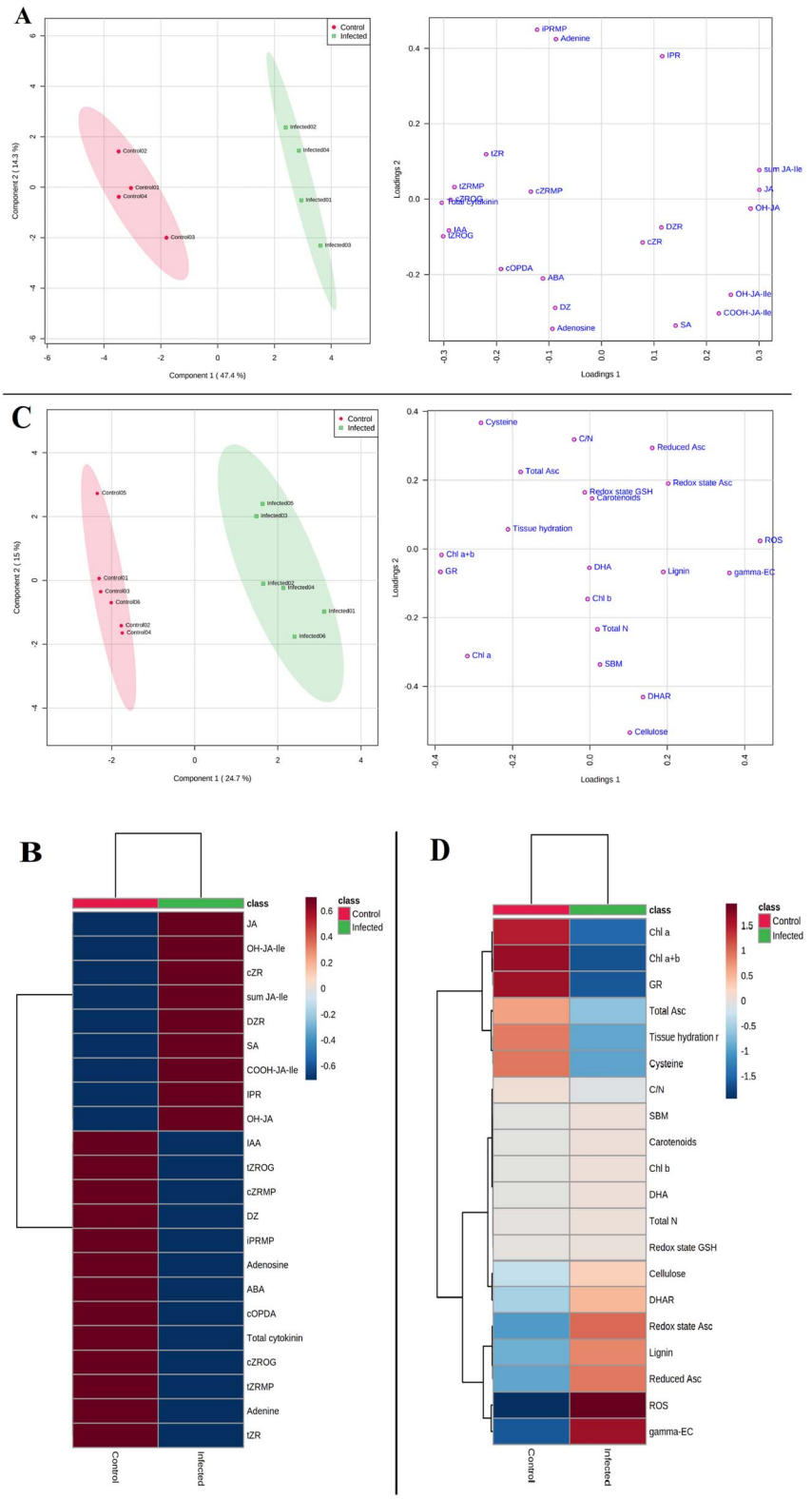

Figure 3. Partial least squares-discriminant analyses (PLS-DA), loading plot diagrams and hierarchical cluster analyses (HCA) with heatmaps of phytohormone profiles, primary metabolites, pigments, cell wall compounds and components of the antioxidant system detected in needles of pine saplings of *D. sapinea* infection and non-infected controls. (A) PLS-DA and its loading plot diagrams of phytohormone profiles; (B) HCA with heatmap of phytohormone profiles; (C) PLS-DA and its loading plot diagrams of metabolites, pigments, cell wall components and the antioxidant system; (D) HCA with heatmap of metabolites, pigments, cell wall components and the antioxidant system in non-infected controls and infected needles.

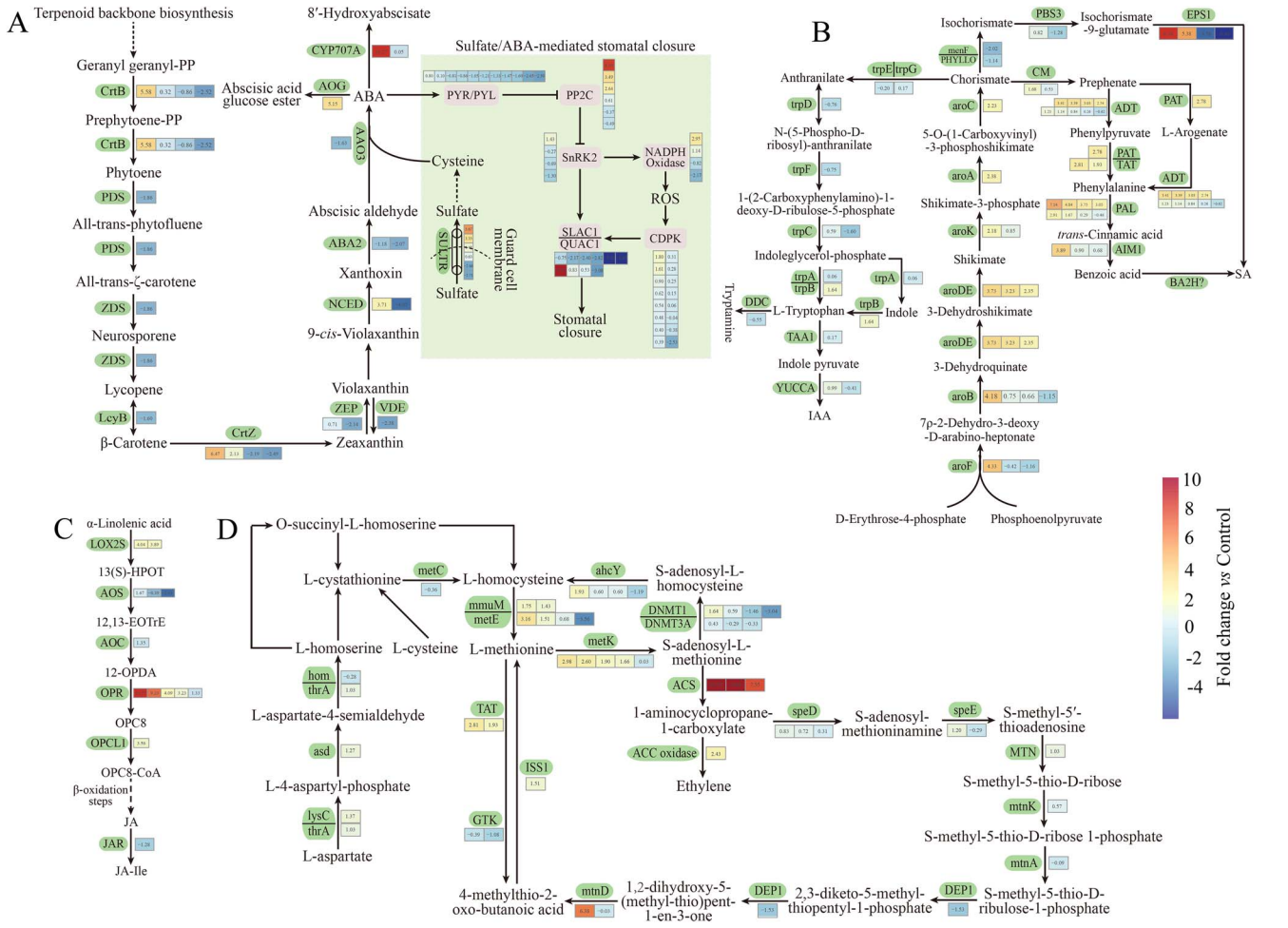

Figure 4. Differentially expressed genes (DEGs) and metabolites involved in phytohormone biosynthesis in pine needles following *D. sapinea* infection. Enzymes are indicated in uppercase letters. Heat map of ABA, IAA, SA, JA and ethylene pathway-related gene expression and values are presented as fold changes relative to controls. (A) ABA pathway. crtB, 15-cis-phytoene synthase; PDS, 15-cis-phytoene desaturase; ZDS, zeta-carotene desaturase; LcyB, lycopene beta-cyclase; CrtZ, β-carotene 3-hydroxylase; ZEP, zeaxanthin epoxidase; VDE, violaxanthin de-epoxidase; NCED, 9-*cis*-epoxycarotenoid dioxygenase; ABA2, xanthoxin dehydrogenase; AAO3, abscisic-aldehyde oxidase; AOG, abscisate beta-glucosyltransferase; CYP707A, ABA 8′-hydroxylase; SULTR, sulfate transporter; PYR/PYL, PYRABACTIN RESISTANCE/PYR1-LIKE; PP2C, protein phosphatase 2C; SnRK2, sucrose nonfermenting 1 (SNF1)-related protein kinase 2; SLAC1, slow anion channel 1; QUAC1, quick anion channel 1; CDPK, calcium-dependent protein kinase. (B) Possible biosynthesis routes for IAA and SA in plants. aroF, 3-deoxy-7-phosphoheptulonate synthase; aroB, 3-dehydroquinate synthase; aroDE, 3-dehydroquinate dehydratase; aroK, shikimate kinase; aroA, 3-phosphoshikimate 1-carboxyvinyltransferase; aroC, chorismate synthase; menF, isochorismate synthase; PHYLLO, protein PHYLLO, chloroplastic; trpE, anthranilate synthase component 1; trpG, anthranilate synthase component 2; trpD, anthranilate phosphoribosyltransferase; trpF, N-(5′-phosphoribosyl)anthranilate isomerase; trpC, indole-3-glycerol phosphate synthase; trpA, tryptophan synthase alpha chain; trpB, tryptophan synthase beta chain; TAA1, L-tryptophan-pyruvate aminotransferase 1; YUCCA, tryptophan aminotransferase; DDC, aromatic-L-amino-acid decarboxylase; PBS3, avrPphB SUSCEPTIBLE3; EPS1, enhanced pseudomonas susceptibility 1; CM, chorismate mutase; ADT, arogenate dehydratase; PAT, prephenate-aminotransferase; TAT, tyrosine aminotransferase; PAL, phenylalanine ammonialyase; AIM1, abnormal inflorescence meristem 1; BA2H, benzoic acid 2-hydroxylas. (C) JA biosynthesis. LOX2S, lipoxygenase; AOS, allene oxide synthase; AOC, allene oxide cyclase; OPR, 12-oxophytodienoate reductase; OPCL1, OPC-8:0 CoA ligase 1, JAR, jasmonate resistant. (D) Ethylene metabolism. thrA, bifunctional aspartokinase; lysC, aspartate kinase; asd, aspartate-semialdehyde dehydrogenase; hom, homoserine dehydrogenase; metC, cysteine-S-conjugate beta-lyase; ahcY, adenosylhomocysteinase; mmuM, homocysteine S-methyltransferase; metE, 5-methyltetrahydropteroyltriglutamate-homocysteine methyltransferase; metK, S-adenosylmethionine synthetase; TAT, tyrosine aminotransferase; GTK, L-glutamine-4-(methylsulfanyl)-2-oxobutanoate aminotransferase; ISS1, aromatic aminotransferase; NMT1, DNA (cytosine-5)-methyltransferase 1; DNMT3A, DNA (cytosine-5)-methyltransferase 3A; ACS, 1-aminocyclopropane-1-carboxylate synthase; ACC oxidase, aminocyclopropanecarboxylate oxidase; cysK, cysteine synthase; ATCYSC1, L-3-cyanoalanine synthase/cysteine synthase; cysE, serine O-acetyltransferase; speD, S-adenosylmethionine decarboxylase; speE, spermidine synthase; MTN, 5′-methylthioadenosine nucleosidase; mtnK, 5-methylthioribose kinase; mtnA, methylthioribose-1-phosphate isomerase; DEP1, methylthioribulose 1-phosphate dehydratase/enolase-phosphatase E1; mtnD, 1,2-dihydroxy-3-keto-5-methylthiopentene dioxygenase.

levels and activities of central antioxidative enzymes were analyzed. PLS-DA based on a total of 25 physiological parameters revealed a distinct clustering pattern between infected needles and needles of control plants (Figure 3C). A similar clustering of physiological and biochemical parameters was observed by HCA (Figure 3D). These results show that *D. sapinea* infection

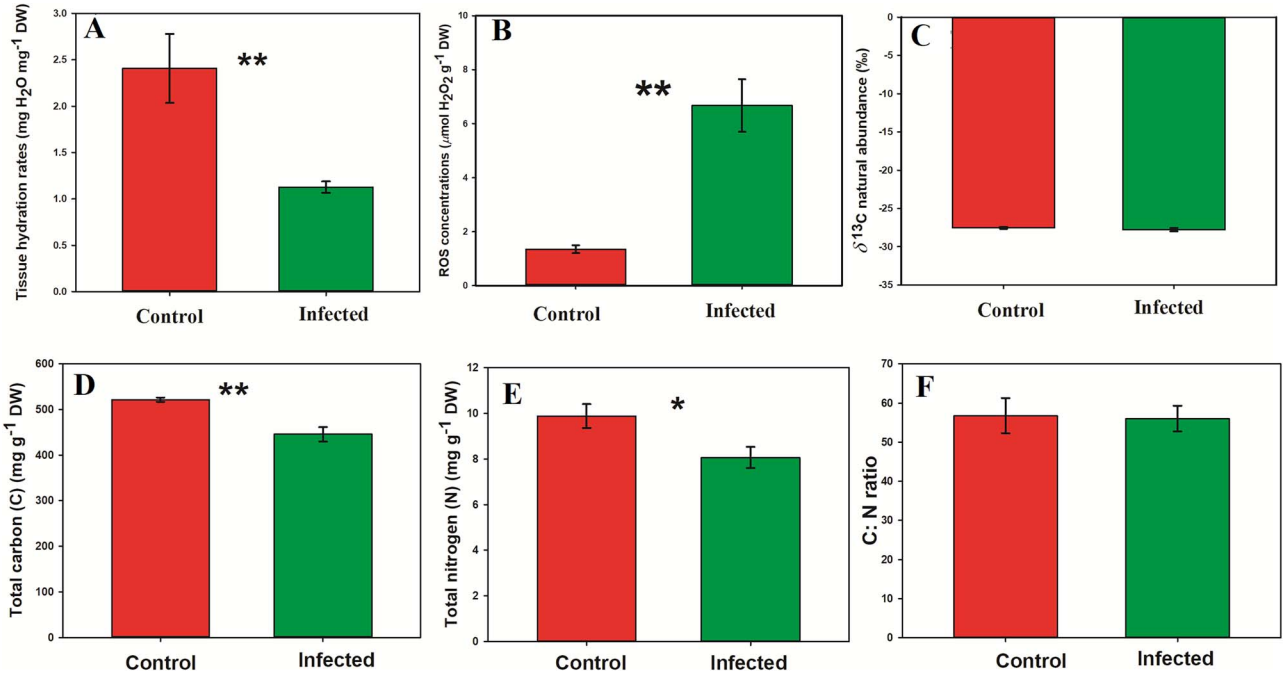

Figure 5. Tissue hydration status (A), reactive oxygen species (ROS: H_2O_2) levels (B), $\delta^{13}C$ abundance (C), total carbon (D), nitrogen (E) levels and carbon/nitrogen ratio (F) in needles of *D. sapinea* infection and non-infected control plants. Columns show means (±SE). Bold asterisks represent significant differences between control and *D. sapinea*-infected leaves at $P < 0.05$. *$0.01 < P < 0.05$ **$0.001 < P < 0.01$.

also induced dominant local changes of foliar structure and metabolism of its pine hosts (Figure 3C and D).

Tissue hydration, as an indicator of current water balance, was impaired in *D. sapinea*-infected needles compared with controls after 7 days post-infection (Figure 5A; Table S2 available as Supplementary data at *Tree Physiology* Online). Still stable carbon isotopes $\delta^{13}C$ natural abundance, an indicator of long-term water balance at undisturbed photosynthesis, was not affected by the fungal invader. *Diplodia sapinea* infection significantly reduced SBM, total nitrogen and carbon contents of *D. sapinea*-infected needles indicating reduced assimilation (see below). However, the carbon:nitrogen ratio of the needles was maintained at *D. sapinea* infection (Figure 5F; Table S2 available as Supplementary data at *Tree Physiology* Online).

In infected needles, a marked accumulation of the lignin is consistent with the gene regulation in the phenylpropanoid pathway involved in lignin biosynthesis (Figure 6; Table S2 available as Supplementary data at *Tree Physiology* Online). In contrast to lignin, cellulose levels were dramatically reduced in the infected needles which is in line with the downregulation of cellulose synthase (*CESA*) and the upregulation of beta-glucosidase (Figure 6).

***Diplodia sapinea* infection affects the biosynthesis of photosynthetic pigments** Levels of several photosynthetic pigments, such as chlorophyll *a*, chlorophyll *b* and carotenoids (Car) showed significantly reduced patterns in *D. sapinea*-infected needles (Figure 7B; Table S2 available as Supplementary data at *Tree Physiology* Online). Transcriptome analysis revealed that both, chlorophyll synthase (*i.e., ChlG*) and chlorophyllase (*i.e., CLH*) are downregulated in the infected samples (Figure 7). In addition, the expression of a substantial number of genes assigned to the photosynthetic pigment biosynthesis route was inhibited (Figure 7).

Reactive oxygen species scavenging and antioxidant activities are reprogrammed by D. sapinea infection Our metabolite analysis revealed strongly enhanced accumulation of the ROS (H_2O_2) in *D. sapinea*-infected needles (Figure 5B). This increase was accompanied by dramatically increased contents of total GSH and reduced GSH and their precursor γ-glutamyl-cysteine (γ-EC). Also oxidized glutathione (GSSG) contents were enhanced, inducing more oxidized redox state of glutathione in the infected needles (Figure 8; Table S3 available as Supplementary data at *Tree Physiology* Online). The increased GSSG level could be attributed to a reduced GR activity (Table S3 available as Supplementary data at *Tree Physiology* Online). Conversely, the reduced and total ascorbate as well as dehydroascorbate (DHA) contents and the ascorbate redox state of the needles were not affected by the *D. sapinea* infection (Table S4 available as Supplementary data at *Tree Physiology* Online). These results are consistent with the unaffected DHAR activity in the infected needles (Table S4 available as Supplementary data at *Tree Physiology* Online). Despite these differences in GSH and ascorbate metabolism, unchanged gene expression was observed in the biosynthesis pathways

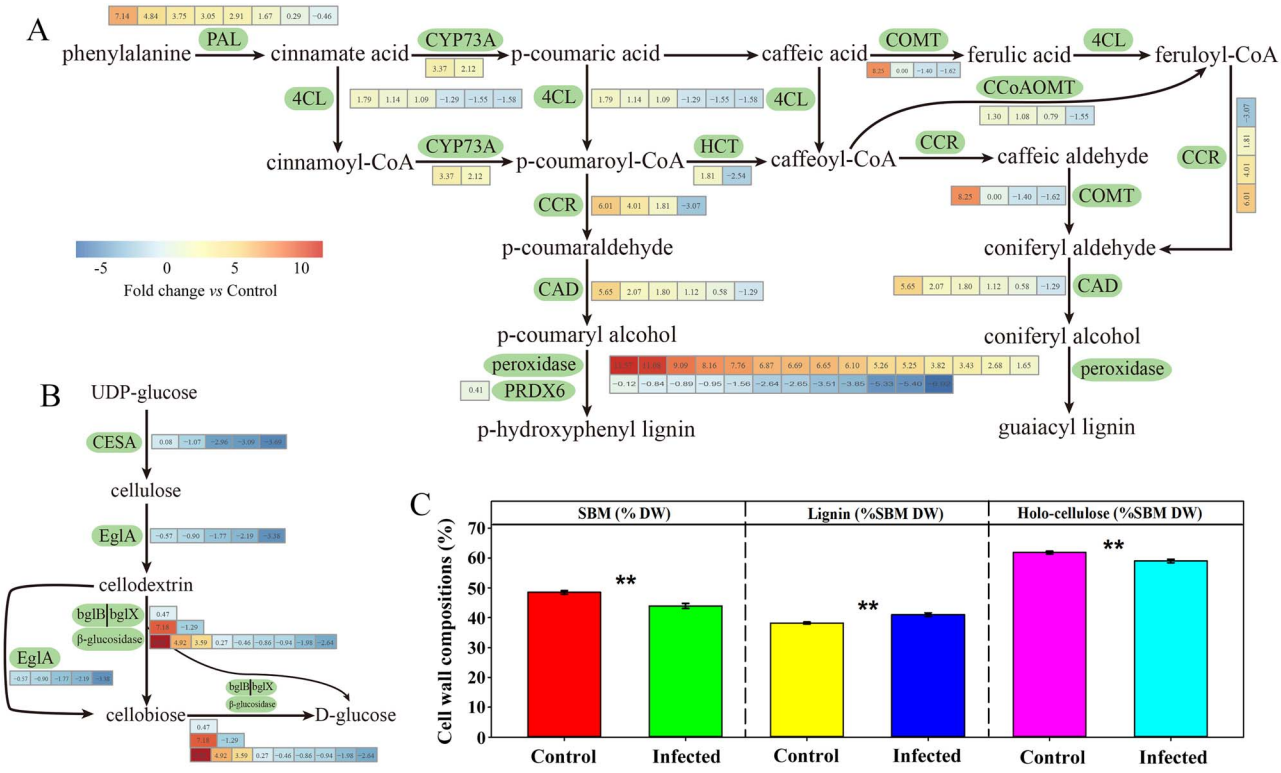

Figure 6. Differentially expressed genes (DEGs) and metabolites involved in lignin and cellulose biosynthesis in pine needles following *D. sapinea* infection. Enzymes are indicated in uppercase letters. Heat map of phenylpropanoid and cellulose pathway-related gene expression and values are presented as fold changes relative to controls. (A) Phenylpropanoid pathway. PAL, phenylalanine ammonia-lyase; CYP73A, *trans*-cinnamate 4-monooxygenase; COMT, caffeic O-methyltransferase; 4CL, 4-coumarate: CoA ligase; HCT, *N*-hydroxycinnamoyl transferase; CCR, cinnamoyl-CoA reductase; CAD, cinnamoyl alcohol dehydrogenase; PRDX6, peroxiredoxin 6. (B) Cellulose pathway. CESA, cellulose synthase a; EglA, β-1,4-endoglucanase; bglB, β-glucosidase; bglX, β-glucosidase. (C) Comparison of cell wall compositions (SBM, lignin and holo-cellulose) between controls and infected pine needles. Columns show means (±SE). Bold asterisks represent significant differences between control and *D. sapinea*-infected leaves at $P < 0.05$.

of both metabolites indicating post-transcriptional regulation of glutathione biosynthesis (Figures 7A and 8B). However, the expression of three enzymes of GSH consumption was upregulated irrespective of glutathione accumulation, *i.e.,* glutathione S-transferases (*GST*), gamma-glutamyltranspeptidase (*GGT1_5*) and Peroxiredoxin (*PRX1*) (Figure 8A). In addition, the transcripts of 15 peroxidases that catalyze the oxidation of phenolic and non-phenolic aromatic compounds with ROS were dramatically upregulated in infected needles.

Discussion

In this study, global profiling of phytohormone contents and the abundance of the associated transcriptome revealed changes in ABA, CKs, IAA, JA, SA and ethylene levels as major responses of pine needles to *D. sapinea* infection, regulated at the level of gene expression. To the best of our knowledge, this is the first report on stress-induced responses of phytohormone profiles in needles of a conifer host infected with a pathogenic fungus. Significant changes of the phytohormone profiles observed in our results confirm that *D. sapinea* infection causes similar host stressful response patterns as drought (Arango-Velez et al. 2016), in line with our hypotheses (i) and (ii) as well as with previous reports (Hu et al. 2018, 2021), particularly for elevated levels of ABA, SA, JA-Ile, JA and its derivatives.

Phytohormones, such as CKs (Walters and McRoberts 2006), ABA (Ton et al. 2009) and IAA (Kazan and Manners 2009), are traditionally known to regulate plant growth and development. In addition, they play vital roles in functioning of the plant immune signaling network. For example, ABA may inhibit the fungal pathogen entry into the needles via stomatal closure, a mechanism even more important in response to low water availability. This view is consistent with the observed elevated ABA level mediated by gene expression–controlled induction of biosynthesis in response to *D. sapinea* infection. The present results may suggest a possible novel role of IAA signaling and senescence induction in plant defense responses to necrotrophic fungi such as *D. sapinea*. However, this conclusion needs further analyses by expression pattern experiment, *e.g.,* using an RT-PCR approach. The enhanced gene expression of *AUX1* and *SAUR* affects auxin levels by altering auxin transport (Ren and Gray 2015, Xu et al. 2017). Therefore, the induction of *AUX1* and *SAUR* genes may explain the reduced IAA levels of *D. sapinea*-infected needles attributed to the enhanced IAA

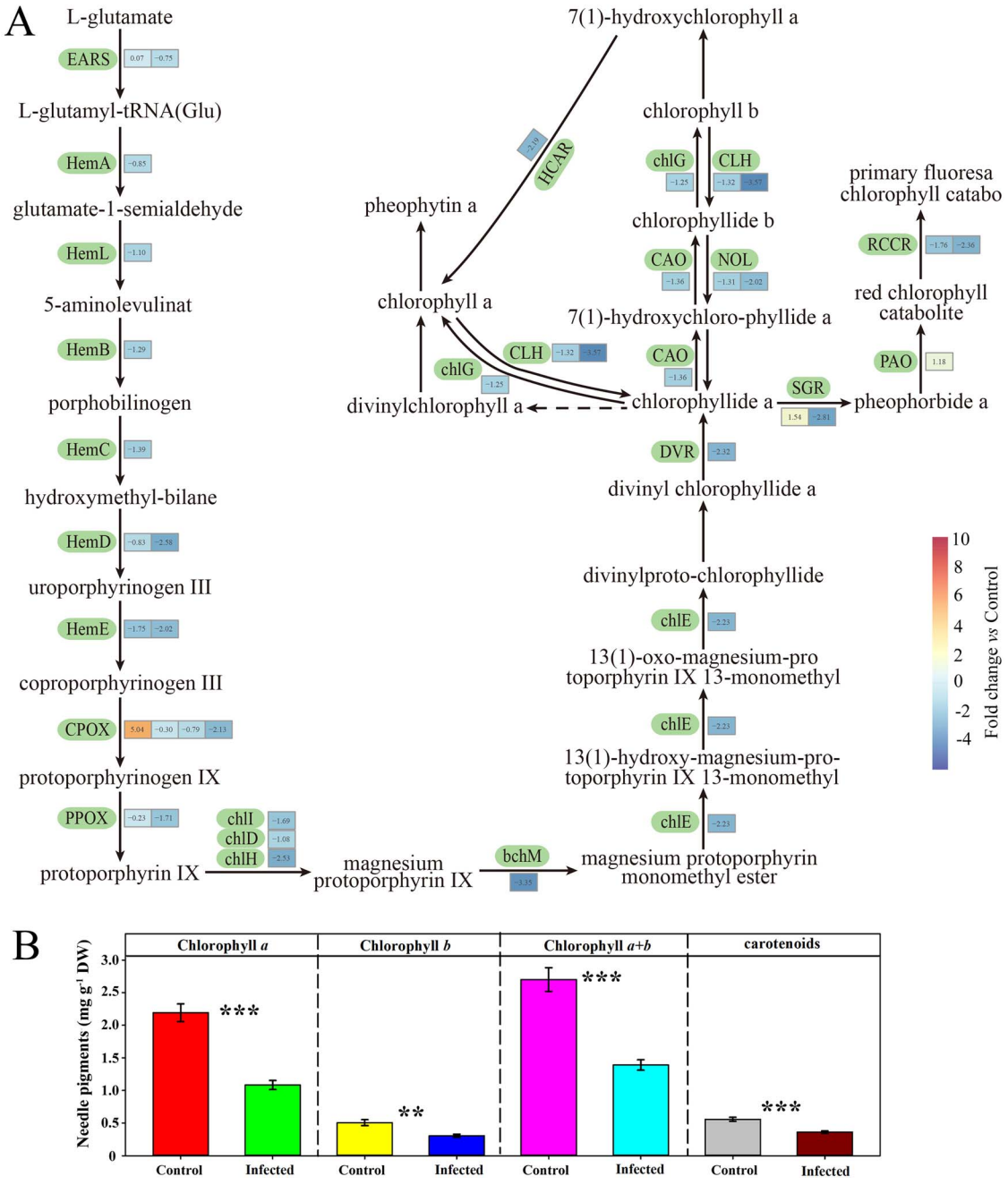

Figure 7. Differentially expressed genes (DEGs) and metabolites involved in the chlorophyll metabolism in pine needles following *D. sapinea* infection. Enzymes are indicated in uppercase letters. Heat map of phenylpropanoid and cellulose pathway–related gene expression and values are presented as fold changes relative to controls. (A) Chlorophyll biosynthesis pathway. EARS, glutamyl-tRNA synthetase; hemA, glutamyl-tRNA reductase; hemL, glutamate-1-semialdehyde 2,1-aminomutase; hemB, porphobilinogen synthase; hemC, hydroxymethylbilane synthase; hemD, uroporphyrinogen-III synthase; hemE, uroporphyrinogen decarboxylase; CPOX, coproporphyrinogen III oxidase; PPOX, protoporphyrinogen/coproporphyrinogen III oxidase; chlI, magnesium chelatase subunit I; chlD, magnesium chelatase subunit D; chlH, magnesium chelatase subunit H; bchM, magnesium-protoporphyrin O-methyltransferase; chlE, magnesium-protoporphyrin IX monomethyl ester (oxidative) cyclase; DVR, divinyl chlorophyllide a 8-vinyl-reductase; CAO, chlorophyllide a oxygenase; NOL, chlorophyll(ide) b reductase; chlG, chlorophyll/bacteriochlorophyll a synthase; CLH, chlorophyllase; HCAR, 7-hydroxymethyl chlorophyll a reductase; SGR, magnesium dechelatase; PAO, pheophorbide a oxygenase; RCCR, red chlorophyll catabolite reductase. (B) Comparison of needle pigments (chlorophyll a, chlorophyll b, chlorophyll a + b and carotenoids) between controls and infected pine needles. Columns show means (±SE). Bold asterisks represent significant differences between control and *D. sapinea*-infected leaves at $P < 0.05$.

export. In addition, previous studies showed that overexpression lines of *SAUR* genes exhibited an early senescence phenotype (Hou et al. 2013, Bemer et al. 2017); a delayed leaf senescence phenotype was observed in loss-of-function mutations in *SAUR* genes (Hou et al. 2013). These observations suggest a senescence-inducing function of *SAUR* genes that

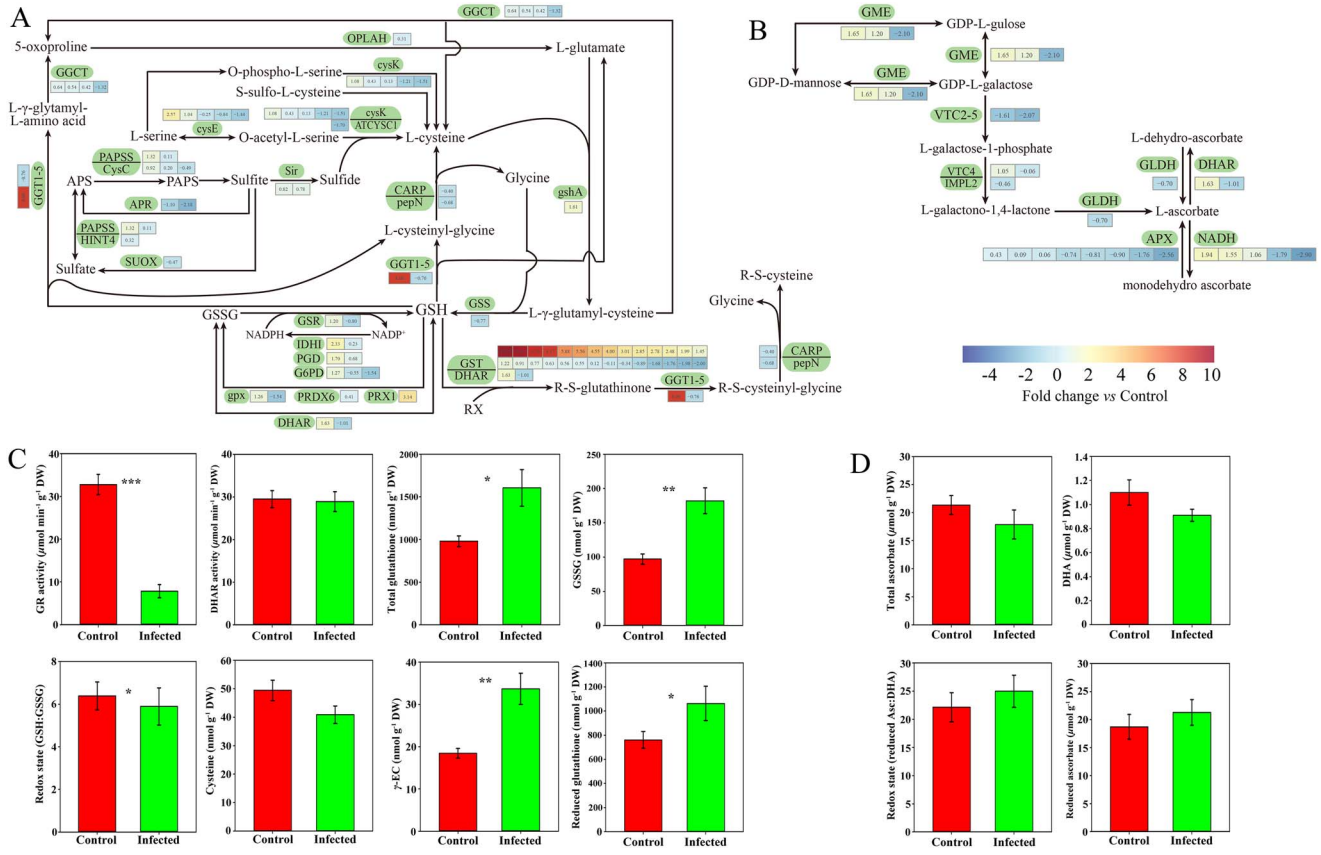

Figure 8. Differentially expressed genes (DEGs) and metabolites involved in antioxidant metabolism in pine needles following *D. sapinea* infection. Enzymes are indicated in uppercase letters. Heat map of GSH and ascorbic acid metabolism-related gene expression and values are presented as fold changes relative to controls. (A) Glutathione pathway. PAPSS, 3′-phosphoadenosine-5′-phosphosulfate synthase; APS, adenosine 5′-phosphosulfate; PAPS, 3-phosphoadenosine 5-phosphosulfate; HINT4, bifunctional adenosine 5′-phosphosulfate phosphorylase/adenylylsulfatase; CysC, adenylyl-sulfate kinase; APR, adenosine 5′-phosphosulphate reductase; SUOX, sulfite oxidase; sir, sulfite reductase; cysE, serine acetyltransferase; cysK, cysteine synthase a; ATCYSC1, cysteine synthase; GGCT, γ-glutamylcyclotransferase; OPLAH, 5-oxoprolinase (ATP-hydrolyzing); CARP, leucyl aminopeptidase; pepN, aminopeptidase N; gshA, glutamate-cysteine ligase; GGT1–5, γ-glutamyltranspeptidase; GSS, glutathione synthase; GSR, glutathione reductase (NADPH); IDH1, isocitrate dehydrogenase; PGD, 6-phosphogluconate dehydrogenase; G6PD, glucose-6-phosphate 1-dehydrogenase; gpx, glutathione peroxidase; PRDX6, peroxiredoxin 6; PRX1, glutaredoxin/glutathione-dependent peroxiredoxin; DHAR, dehydroascorbate reductase; GST, glutathione S-transferase. (B) Ascorbic acid pathway. GME, GDP-D-mannose 3′, 5′-epimerase; VTC2–5, GDP-L-galactose phosphorylase; VTC4, inositol-phosphate phosphatase; IMPL2, histidinol-phosphatase; GLDH, L-galactono-1,4-lactone dehydrogenase; APX, L-ascorbate peroxidase; NADH, ubiquinone oxidoreductase. (C) Comparison of GR activity, glutathione dehydrogenase (DHAR) activity, total glutathione (GSH), glutathione disulfide (GSSG), cysteine, γ-glutamylcysteine (γ-EC), reduced glutathione and redox state (GSH: GSSG) between control and infected pine needles. (D) Comparison of total ascorbate (Asc), dehydroascorbate (DHA), reduced ascorbate and redox state (reduced Asc:DHA) between controls and infected pine needles. Columns show means (±SE). Bold asterisks represent significant differences between control and *D. sapinea*-infected leaves at $P < 0.05$.

is probably regulated by interaction with a *PP2C.D* phosphatase (Xiao et al. 2015). Thus, in this study, we assume that enhanced expression of *SAUR* genes may be responsible for the observed early senescence and cellular suicide of pine needles in response to *D. sapinea* infection. In contrast, both possible biosynthesis routes for SA in plants, *i.e.,* the isochorismate and phenylalanine pathways (Peng et al. 2021), were activated to contribute to SA accumulation in infected pine needles.

In general, changes of the antioxidative system constitute defense reactions aimed to keep ROS in safe levels under biotic stress (Foyer and Rennenberg 2000, Foyer and Noctor 2011). The responses of the antioxidative system induced by the *D. sapinea* infection were also observed in infected needles of the pine host of current study. However, these changes can be interpreted as unsuccessful defense. Enhanced glutathione (GSH) synthesis as defense reaction to the fungal infection was achieved, but counteracted by decreased GR activity, apparently both by post-transcriptional control. Consequently, GSSG accumulation and a more oxidized redox state of glutathione as well as elevated H_2O_2 levels were observed. This response of the antioxidative system of infected pine needles is consistent with both, local responses in the bark and wood, and systemic responses of non-infected pine needles in *D. sapinea*-infected pine trees (Hu et al. 2018, 2021). The upregulated expression of enzymes involved in GSH consumption, *i.e., GST*, *GGT1_5* and *PRX1*, may have contributed to a limitation of GSH availability for ROS scavenging. The similar patterns of redox state of GSH have previously been reported as the HR to pathogen

infection, subsequently resulting in the PCD (Foyer and Noctor 2011). In our results, necrosis of the terminal shoot that spreads through the entire host plant with increasing fungal exposure, reflecting the typical symptoms of infection with necrotrophic *D. sapinea* (Oliva et al. 2014, Sherwood et al. 2015).

As previously reported for the systemic response of non-infected needles and roots of infected pine hosts (Hu et al. 2021), JA and its derivatives OH-JA, OH-JA-Ile and COOH-JA-Ile were not detected in controls, but only in infected needles. This result indicates local induction of biosynthesis of JA class phytohormones in response to *D. sapinea* infection as a defense reaction. It is well documented that JA signaling is responsible to necrotrophic pathogen attack, whereas SA signaling constitutes a response to biotrophic and hemi-biotrophic pathogens attacks (Glazebrook 2005, Robert-Seilaniantz et al. 2011). Thus, our results agree with the opinion that JA is rapidly synthesized from linolenic acid upon *D. sapinea* infection and, subsequently, metabolized to JA-Ile, the active form of JA. Since the transcripts of genes coding for *JASMONATE RESISTANT (JAR)* were not detected in our samples, it is assumed that the induction of the biosynthesis of JA class phytohormones is an early response to *D. sapinea* infection. To confirm this assumption, quantification of JA pathway components and the associated transcriptome in a time-course approach is required in future studies of responses to *D. sapinea* infection.

Although the interplay between SA and JA is well-documented in plant–pathogen relationships, the increased levels of SA in the present results (+ ~12-fold) in *D. sapinea*-infected needles constitutes new information for the response to a necrotrophic invader and show the complex interactions of SA–JA signaling pathways during pathogen invasion (Koornneef and Pieterse 2008, Hu et al. 2018). In addition, the enhanced SA level observed in infected needles is in line with the systemic response observed in non-infected needles and roots of pine plants upon infection by *D. sapinea* (Hu et al. 2021). This result suggests that long-distance transport of SA out of *D. sapinea*-infected needles may be responsible for the systemic accumulation of this phytohormone in non-infected tissues (Hu et al. 2021). Time courses of xylem sap and phloem exudate analyses are required in future studies to test this assumption.

Consistent with an impaired water status in bark and wood organs of *D. sapinea*-infected Scots pine hosts in the field (Hu et al. 2018), reduced hydration of infected needles was observed in our results with pine saplings (hypothesis (ii)). To determine whether *D. sapinea* infection triggered corresponding transcriptomic response that resemble drought, we examined the expression pattern of genes involved in stomatal movement (Malcheska et al. 2017, Batool et al. 2018). It has been shown that sulfate is a central signal of drought that induces stomatal closure via anion channels (*i.e., QUAC1*/*ALMT12* and *SLAC1*) and/or guard cell ABA synthesis. Our results showed that the expression of a sulfate transporter *SULTR*, responsible for sulfate uptake, significantly increased at 7 days post-infection. Sulfate taken up into guard cells is supposed to upregulate the expression of *NCED*, a key step of ABA synthesis, thereby leading to elevated ABA concentration in the guard cell cytosol. Coincidentally, our transcriptomic analysis showed that *NCED* was almost 13-fold upregulated upon pathogen exposure. Sulfate is also proposed to gate both the R-Type anion channel *QUAC1* and S-type anion channel *SLAC1* under drought stress. However, in this present study, the highly activated *QUAC1* showed a contrasting expression pattern with *SLAC1*, indicating a differential role of these two anion channels in pathogen-induced water deficit response. We also scrutinized the gene expression of potassium outward channels *GORK*, which can mediate stomatal turgor loss and, consequently, stomatal closure. However, *GORK* was not significantly affected by pathogen infection (data not shown). These finding collectively suggested that *D. sapinea* infection has led to similar, but not to identical transcriptomic responses as to drought in pine needles. Nevertheless, the present result is surprising since the enhanced ABA accumulation should have prevented extensive water loss by stomatal closure. However, it is still unclear which processes determine water loss from the infected needles, since pathogens may have evolved specific virulence factors, such as coronatine that effectively re-opens stomata as an important pathogenesis strategy to counteract stomatal closure (Melotto et al. 2006, Zheng et al. 2012).

In this study, the impaired water status was observed with the decrease of photosynthetic pigments suggesting a reduced photosynthesis. The remaining photosynthetic pigments may not only be responsible for the light energy absorbing (Gough et al. 2003, Tanaka et al. 2011), but together with their breakdown products may also function as a defense against necrotrophic *D. sapinea* because of the toxicity to the cells of pathogen (Kariola et al. 2005, Hu et al. 2015). This function may be even more important in the systemic response to *D. sapinea* infection, where increased rather than reduced levels of photosynthetic pigments were observed in non-infected needles of pine plants (Hu et al. 2021). Combined with the enhanced ROS (H_2O_2) levels, the present results indicate that local needle damages caused by necrotrophic *D. sapinea* include the release of chlorophylls from chloroplasts thylakoid membranes of infected tissue. This will accelerate ROS production, particularly since rapid degradation seems to be downregulated in infected needles as indicated by reduced gene expression of chlorophyllase.

Necrotrophic pathogens retrieve nutrients from dead plant cells, which requires the breakdown of plant cell walls and tissue structures (Oliva et al. 2014). The reduced portion of SBM on DW observed in our results is a consequence of such breakdown and consistent with the findings in both, systemic non-infected tissues of pine saplings (Hu et al. 2021) as well as tissues of pine trees in the field (Hu et al. 2018). The reduction of SBM

in host tissues prepares the ground for successful penetration by *D. sapinea* fungus, because cell walls constitute an essential physical defense upon pathogen infection (Hématy et al. 2009, Oliva et al. 2014, Sherwood and Bonello 2016). Transcriptome and metabolome analyses in this study indicate that reprogramming of the phenylpropanoid pathway with increased lignin formation at the expense of cellulose constitutes a defense reaction to the *D. sapinea* infection (hypothese (iii) and (iv)). Apparently, the pine host retrieves carbon from SBM by cellulose degradation for enhanced lignin synthesis, in line with other fungus attacks (*e.g.,* Ahamed and Ahring 2011). Active lignification has been well documented as a defense reaction of plants upon pathogen infection (Glazebrook 2005) and was observed in both in vivo and in vitro experiments as systemic induced response of Austrian pine against *D. sapinea* attack (Bonello and Blodgett 2003, Blodgett et al. 2007). Increased lignification, as observed in our results in *D. sapinea*-infected Scots pine needles, was also observed in other necrotrophic and biotrophic fungi (Smith et al. 2007, Zhang et al. 2007, Hu et al. 2017), such as Austrian pine infected by *Diplodia scrobiculata* in vivo (Blodgett et al. 2007, Wallis et al. 2008, Sherwood and Bonello 2016). Also in vitro studies indicate that lignification plays an essential role in the response of its host against *D. sapinea* (Celimene et al. 2001, Sherwood and Bonello 2013). However, the present results clearly show that enhanced lignification of the cell walls of pine needles was insufficient to prevent *D. sapinea* invasion.

In this context, changes of lignification processes in our results could be recognized as the consequence of plant–pathogen interactions mediated by the plant hormonal signaling cascades, particularly of CKs (Nafisi et al. 2015). Consistent with such assumption, our results show enhanced levels of CKs including their bioactive forms (*i.e.,* DZ, iPR, tZR, iPRMP) and inactive forms for storing (*i.e.,* cZR, DZR) as well as its precursor, adenine, in *D. sapinea*-infected needles. The accumulated foliar CKs are in line with systemic enhanced levels of CKs in non-infected needles of pine saplings infected by *D. sapinea* (Hu et al. 2021). In previous studies, elevated CKs levels were related to enhanced resistance to necrotrophic fungi infection in tomato infected by *Botrytis cinerea* (Swartzberg et al. 2008) and *Arabidopsis* infected by *Alternaria brassicicola KACC40036* Choi et al. (2011). Therefore, changes in composition of SBM, *e.g.,* cellulose and lignin, in response to *D. sapinea* infection could relate to the changes of CKs levels (Nafisi et al. 2015). However, the function of CKs in plants in response to pathogen attacks still needs to be elucidated in future study (Bari and Jones 2009).

In summary, our results indicate that successful *D. sapinea* attack of pine needles depends on (a) reprogramming of the host's phytohormone synthesis and crosstalk towards early senescence by gene expression despite the induction of defense reactions; (b) enhanced ROS production, *e.g.,* during the degradation of photosynthetic pigments; (c) counteracting enhanced ROS scavenging via elevated glutathione (GSH) synthesis by reducing the regeneration of this antioxidant at the post-transcriptional level; (d) disturbing the foliar water balance by de-regulating stomatal aperture; and (e) enhancement of foliar cell wall barriers by stimulated lignification through gene expression, but only to an extent insufficient to prevent fungal invasion. Thus, the induction of combined changes of transcriptional and post-transcriptional processes in host tissues appears to overcome the defense reactions of host tissues and mediate successful invasion of pine needles and its cellular suicide by necrotrophic *D. sapinea*.

Supplementary data

Supplementary data for this article are available at *Tree Physiology* Online.

Data and materials availability

All data needed to evaluate the conclusions in the paper are present in the paper and/or the Supplementary Materials. Raw next-generation sequencing read sequences have been deposited at the National Center for Biotechnology Information under Bioproject ID PRJNA756102 (http://www.ncbi.nlm.nih.gov/bioproject/756102).

Acknowledgments

We express special thanks to Cornelia Blessing (Universität of Freiburg, Freiburg, Germany), Barbara Kettig and Dagmar Böhmert (IPK, Gatersleben, Germany) for excellent technical assistance. The authors also acknowledge Monika Eiblmeier for her comments on the experimental design and support during the use of laboratory facilities in Freiburg, Germany.

Conflict of interest

The authors declare that they have no competing interests.

Funding

This study was part of the WAHYKLAS project (No. 28WC403105) funded via the Bundesanstalt für Landwirtschaft und Ernährung (BLE), Germany, by the Bundesministerium für Ernährung und Landwirtschaft (BMEL) and the Bundesministerium für Umwelt, Naturschutz, Bau und Reaktorsicherheit (BMUB), Germany, based on the decision of the German Federal Parliament. Financial support of the 'Double-First Class' Initiative Program for Foreign Talents of Southwest University and the 'Prominent Scientist Program' of Chongqing Talents (cstc2021ycjh-bgzxm0002 & cstc2021ycjh-bgzxm0020), China is gratefully acknowledged.

Authors' contributions

B.H. and H.R. designed research; B.H., A.M., B.V., F.S.P. and N.W. performed research; B.H., ZhSh.L. R.H. and M.M. analyzed data; and B.H., ZhSh.L., K.M. and H.R. wrote the paper.

References

Ahamed A, Ahring BK (2011) Production of hydrocarbon compounds by endophytic fungi *Gliocladium* species grown on cellulose. Bioresour Technol 102:9718–9722.

Andrews S (2014) FastQC a quality control tool for high throughput sequence data. https://github.com/s-andrews/FastQC

Arab L, Kreuzwieser J, Kruse J et al. (2016) Acclimation to heat and drought – lessons to learn from the date palm *Phoenix dactilyfera*. Environ Exp Bot 125:20–30.

Arango-Velez A, El Kayal W, Copeland CC, Zaharia LI, Lusebrink I, Cooke JE (2016) Differences in defense responses of *Pinus contorta* and *Pinus banksiana* to the mountain pine beetle fungal associate *Grosmannia clavigera* are affected by water deficit. Plant Cell Environ 39:726–744.

Bari R, Jones JDG (2009) Role of plant hormones in plant defense responses. Plant Mol Biol 69:473–488.

Batool S, Uslu VV, Rajab H et al. (2018) Sulfate is incorporated into cysteine to trigger ABA production and stomatal closure. Plant Cell 30:2973–2987.

Bemer M, Van Mourik H, Muino JM, Ferrándiz C, Kaufmann K, Angenent GC (2017) FRUITFULL controls SAUR10 expression and regulates Arabidopsis growth and architecture. J Exp Bot 68:3391–3403.

Berger S, Sinha AK, Roitsch T (2007) Plant physiology meets phytopathology: plant primary metabolism and plant–pathogen interactions. J Exp Bot 58:4019–4026.

Blaschke L, Forstreuter M, Sheppard LJ, Leith IK, Murray MB, Polle A (2002) Lignification in beech (*Fagus sylvatica*) grown at elevated CO_2 concentrations: interaction with nutrient availability and leaf maturation. Tree Physiol 22:469–477.

Blodgett JT, Eyles A, Bonello P (2007) Organ-dependent induction of systemic resistance and systemic susceptibility in *Pinus nigra* inoculated with *Sphaeropsis sapinea* and *Diplodia scrobiculata*. Tree Physiol 27:511–517.

Blumenstein K, Bußkamp J, Langer GJ, Langer EJ, Terhonen E (2020) The opportunistic pathogen *Sphaeropsis sapinea* is found to be one of the most abundant fungi in symptomless and diseased scots pine in Central-Europe. PREPRINT (Version 1) available at Research Square. https://doi.org/10.21203/rs.3.rs-48366/v1.

Blumenstein K, Bußkamp J, Langer GJ, Schlößer R, Parra Rojas NM, Terhonen E (2021) *Sphaeropsis sapinea* and associated endophytes in scots pine: interactions and effect on the host under variable water content. Front For Glob Change 4:655769.

Bolger A, Lohse M, Usadel B (2014) Trimmomatic: a flexible trimmer for Illumina sequence data. Bioinformatics 30:2114–2120.

Bonello P, Blodgett JT (2003) *Pinus nigra–Sphaeropsis sapinea* as a model pathosystem to investigate local and systemic effects of fungal infection of pines. Physiol Mol Plant Pathol 63: 249–261.

Bray NL, Pimentel H, Melsted P, Pachter L (2016) Near-optimal probabilistic RNA-seq quantification. Nat Biotechnol 34:525–527.

Brinkmann K, Blaschke L, Polle A (2002) Comparison of different methods for lignin determination as a basis for calibration of near-infrared reflectance spectroscopy and implications of lignoproteins. J Chem Ecol 28:2483–2501.

Brodde L, Adamson K, Julio Camarero J et al. (2019) Diplodia tip blight on its way to the north: drivers of disease emergence in northern Europe. Front Plant Sci 9:1818. https://doi.org/10.3389/fpls.2018.01818.

Burgess TI, Wingfield MJ, Wingfield BD (2004) Global distribution of *Diplodia pinea* genotypes revealed using simple sequence repeat (SSR) markers. Australas Plant Pathol 33:513–519.

Bußkamp J (2018) Schadenserhebung, Kartierung und Charakterisierung des, Diplodia- Triebsterbens der Kiefer, insbesondere des endophytischen Vorkommens in den klimasensiblen Räumen und Identifikation von den in Kiefer (*Pinus sylvestris*) vorkommenden Endophyten. PhD thesis. University of Kassel, Kassel.

Bußkamp J, Langer GJ, Langer EJ (2020) *Sphaeropsis sapinea* and fungal endophyte diversity in twigs of scots pine (*Pinus sylvestris*) in Germany. Mycol Progr 19:985–999.

CABI (2019) *Sphaeropsis sapinea* (Sphaeropsis blight) Invasive species compendium. Available online at: https://www.cabi.org/isc/datasheet/19160 (13 November 2021, date last accessed).

Celimene CC, Smith DR, Young RA, Stanosz GR (2001) In vitro inhibition of *Sphaeropsis sapinea* by natural stilbenes. Phytochemistry 56:161–165.

Choi J, Choi D, Lee S, Ryu CM, Hwang I (2011) Cytokinins and plant immunity: old foes or new friends? Trends Plant Sci 16:388–394.

Dewey CN, Li B (2011) RSEM: accurate transcript quantification from RNA-Seq data with or without a reference genome. BMC Bioinformatics 12:323–323.

Eggert K, von Wirén N (2017) Response of the plant hormone network to boron deficiency. New Phytol 216:868–881.

Fabre B, Piou D, Desprez-Loustau ML, Marcais B (2011) Can the emergence of pine *Diplodia* shoot blight in France be explained by changes in pathogen pressure linked to climate change? Glob Chang Biol 17:3218–3227.

Flowers J, Hartman JR, Vaillancourt LJ (2006) Histology of *Diplodia pinea* in diseased and latently infected *Pinus nigra* shoots. For Pathol 36:447–459.

Foyer CH, Noctor G (2011) Ascorbate and glutathione: the heart of the redox hub. Plant Physiol 155:2–18.

Foyer CH, Rennenberg H (2000) Regulation of glutathione synthesis and its role in abiotic and biotic stress defense. In: Brunold C, Rennenberg H, De Kok LJ, Stulen I, Davidian JC (eds) Sulfur nutrition and sulfur assimilation in higher plants: molecular, biochemical and physiological aspects. Paul Haupt, Bern, pp 127–153.

Gardes M, Bruns TD (1993) ITS primers with enhanced specificity for *basidiomycetes* – application to the identification of mycorrhizae and rusts. Mol Ecol 2:113–118.

Geßler A, Duarte HM, Franco AC, Luettge U, de Mattos EA, Nahm M, Scarano FR, Zaluar HLT, Rennenberg H (2005) Ecophysiology of selected tree species in different plant communities at the periphery of the Atlantic Forest of SE-Brazil II. Spatial and ontogenetic dynamics in *Andira legalis*, a deciduous legume tree. Trees 19: 510–522.

Glazebrook J (2005) Contrasting mechanisms of defense against biotrophic and necrotrophic pathogens. Annu Rev Phytopathol 43:205–227.

Gough SP, Westergren T, Hansson M (2003) Chlorophyll biosynthesis in higher plants. Regulatory aspects of 5-aminolevulinate formation. J Plant Biol 46:135–160.

Gould N, Reglinski T, Northcott GL, Spiers M, Taylor JT (2009) Physiological and biochemical responses in *Pinus radiata* seedlings associated with methyl jasmonate-induced resistance to *Diplodia pinea*. Physiol Mol Plant Pathol 74:121–128.

Grabherr MG, Haas BJ, Yassour M, Levin JZ, Amit I (2013) Trinity: reconstructing a full-length transcriptome without a genome from RNA-Seq data. Nat Biotechnol 29:644–652.

Haberer K, Herbinger K, Alexou M, Tausz M, Rennenberg H (2007) Antioxidative defensce of old growth beech (*Fagus sylvatica*) under

double ambient O_3 concentrations in a free-air exposure system. Plant Biol 9:215–226.
Hématy K, Cherk C, Somerville S (2009) Host–pathogen warfare at the plant cell wall. Curr Opin Plant Biol 12:406–413.
Heyer M, Scholz SS, Voigt D, Reichelt M, Aldon D, Oelmüller R, Boland W, Mithöfer A (2018) Herbivory-responsive calmodulin-like protein CML9 does not guide jasmonate-mediated defenses in Arabidopsis thaliana. PLoS One 13:e0197633, https://doi.org/10.1371/journal.pone.0197633.
Hou K, Wu W, Gan SS (2013) SAUR36, a small auxin up RNA gene, is involved in the promotion of leaf senescence in *Arabidopsis*. Plant Physiol 161:1002–1009.
Hu B, Sakakibara H, Takebayashi Y et al. (2017) Mistletoe infestation mediates alteration of the phytohormone profile and anti-oxidative metabolism in bark and wood of its host *Pinus sylvestris*. Tree Physiol 37:676–691.
Hu B, Sakakibara H, Kojima M et al. (2018) Consequences of Sphaeropsis tip blight disease for the phytohormone profile and anti-oxidative metabolism of its pine host. Plant Cell Environ 41:737–754.
Hu B, Mithöfer A, Reichelt M, Eggert K, Peters FS, Ma M, Schumacher J, Kreuzwieser J, von Wirén N, Rennenberg H (2021) Systemic reprogramming of phytohormone profiles and metabolic traits by virulent Diplodia infection in its pine (*Pinus sylvestris* L.) host. Plant Cell Environ 44:2744–2764.
Hu X, Makita S, Schelbert Set al. (2015) Reexamination of chlorophyllase function implies its involvement in defense against chewing herbivores. Plant Physiol 167:660–670.
Kariola T, Brader G, Li J, Palva ET (2005) Chlorophyllase, a damage control enzyme, affects the balance between defense pathways in plants. Plant Cell 17:282–294.
Kazan K, Manners JM (2009) Linking development to defense: auxin in plant–pathogen interactions. Trends Plant Sci 14:373–382.
Kim D, Langmead B, Salzberg SL (2015) HISAT: a fast spliced aligner with low memory requirements. Nat Methods 12:357–360.
Koornneef A, Pieterse CM (2008) Cross talk in defense signalling. Plant Physiol 146:839–844.
Langer G (1994) Die Gattung Botryobasidium Donk (Corticiaceae, Basidiomycetes). Cramer, Berlin.
Law CW, Chen Y, Shi W, Smyth GK (2014) Voom: precision weights unlock linear model analysis tools for RNA-seq read counts. Genome Biol 15:R29.
Pieterse CMJ, Leon-Reyes A, Van der Ent S, Van Wees SCM (2009) Networking by small-molecule hormones in plant immunity. Nat Chem Biol 5:308–316.
Li W, Godzik A (2006) Cd-hit: a fast program for clustering and comparing large sets of protein or nucleotide sequences. Bioinformatics 22:1658–1659.
Lichtenthaler HK (1987) Chlorophylls and carotenoids: pigments of photosynthetic biomembranes. Methods Enzymol 148:350–382.
Luchi N, Longa O, Danti R, Capretti P, Maresi G (2014) *Diplodia sapinea*: the main fungal species involved in the colonization of pine shoots in Italy. For Pathol 44:372–381.
Malcheska F, Ahmad A, Batoo S et al. (2017) Drought enhanced xylem sap sulfate closes stomata by affecting ALMT12 and guard cell ABA synthesis. Plant Physiol 174:798–814.
Mantoura RFC, Jeffrey SW, Llewellyn CA, Claustre H, Morales CE (1997) Comparison between spectrophotometric, fluorometric and HPLC methods for chlorophyll analysis. In: Jeffrey, SW et al. (ed) Phytoplankton pigments in oceanography: guidelines to modern methods. Monogr Oceanogr Methodol 10, UNESCO:361–380.
Mashiguchi K, Tanaka K, Sakai T et al. (2011) The main auxin biosynthesis pathway in *Arabidopsis*. Proc Natl Acad Sci USA 108:18512–18517.
Melotto M, Underwood W, Koczan J, Nomura K, He S (2006) The innate immune function of plant stomata against bacterial invasion. Cell 126:969–980.
Nafisi M, Fimognari L, Sakuragi Y (2015) Interplays between the cell wall and phytohormones in interaction between plants and necrotrophic pathogens. Phytochemistry 112:63–71.
Oliva J, Stenlid J, Martínez-Vilalta J (2014) The effect of fungal pathogens on the water and carbon economy of trees: implications for drought-induced mortality. New Phytol 203:1028–1035.
Oliva J, Ridley M, Redondo MA, Caballol M (2021) Competitive exclusion amongst endophytes determines shoot blight severity on pine. Funct Ecol 35:239–254.
Oshlack A, Robinson MD, Young MD (2010) From RNA-seq reads to differential expression results. Genome Biol 11:220. https://doi.org/10.1186/gb-2010-11-12-220.
Paez CA, Smith JA (2018) First report of *Diplodia sapinea* and *Diplodia scrobiculata* causing an outbreak of tip blight on slash pine in Florida. Plant Dis 102:1657.
Pang Z, Chong J, Zhou G et al. (2021) MetaboAnalyst 5.0: narrowing the gap between raw spectra and functional insights. Nucleic Acids Res 49:388–396.
Peng Y, Yang J, Li X, Zhang Y (2021) Salicylic acid: biosynthesis and signaling. Annu Rev Plant Biol 72:761–791.
Pieterse CM, Van der Does D, Zamioudis C, Leon-Reyes A, Van Wees SC (2012) Hormonal modulation of plant immunity. Annu Rev Cell Dev Biol 28:489–521.
Polle A, Chakrabarti K, Schürmann W, Rennenberg H (1990) Composition and properties of hydrogen peroxide decomposing systems in extracellular and total extracts from needles of Norway spruce (*Picea abies* L., Karst.). Plant Physiol 94:312–319.
Ren H, Gray WM (2015) SAUR proteins as effectors of hormonal and environmental signals in plant growth. Mol Plant 8:1153–1164.
Robert-Seilaniantz A, Grant M, Jones JD (2011) Hormone crosstalk in plant disease and defense: more than just Jasmonate-salitylate antagonism. Annu Rev Phytopathol 49:317–343.
Robinson MD, McCarthy DJ, Smyth GK (2010) edgeR: a Bioconductor package for differential expression analysis of digital gene expression data. Bioinformatics 26:139–140.
Rojas CM, Senthil-Kumar M, Tzin V, Mysore K (2014) Regulation of primary plant metabolism during plant-pathogen interactions and its contribution to plant defense. Front Plant Sci 5:17.
Rowland AP, Roberts JG (1994) Lignin and cellulose fractionation in decomposition studies using acid-detergent fibre methods. Commun Soil Sci Plant Anal 25:269–277.
Sanger F, Nicklen S, Coulson AR (1977) DNA sequencing with chainterminating inhibitors. Proc Natl Acad Sci USA 74: 5463–5467.
Schumacher J (2012) Auftreten und Ausbreitung neuartiger Baumkrankheiten in Mitteleuropa unter Berücksichtigung klimatischer Aspekte. Ulmer Verlag, Stuttgart, Contributions to Forest Science, p 153.
Schupp R, Rennenberg H (1988) Diurnal changes in the glutathione content of spruce needles (*Picea abies* L.). Plant Sci 57: 113–117.
Sherwood P, Bonello P (2013) Austrian pine phenolics are likely contributors to systemic induced resistance against *Diplodia pinea*. Tree Physiol 33:845–854.
Sherwood P, Bonello P (2016) Testing the systemic induced resistance hypothesis with Austrian pine and *Diplodia sapinea*. Physiol Mol Plant Pathol 94:118–125.
Sherwood P, Villari C, Capretti P, Bonello P (2015) Mechanisms of induced susceptibility to *Diplodia* tip blight in drought-stressed Austrian pine. Tree Physiol 35:549–562.

Simão FA, Waterhouse RM, Panagiotis I, Kriventseva EV, Zdobnov EM (2015) BUSCO: assessing genome assembly and annotation completeness with single-copy orthologs. Bioinformatics 31:3210–3212.

Smith AH, Gill WM, Pinkard EA, Mohammed CL (2007) Anatomical and histochemical defence responses induced in juvenile leaves of *Eucalyptus globulus* and *Eucalyptus nitens* by *Mycosphaerella* infection. For Pathol 37:361–373.

Spoel SH, Dong X (2012) How do plants achieve immunity? Defence without specialized immune cells. Nat Rev Immunol 12:89–100.

Stanosz GR, Blodgett JT, Smith DR, Kruger EL (2001) Water stress and *Sphaeropsis sapinea* as a latent pathogen of red pine seedlings. New Phytol 149:531–538.

Strohm M, Jouanin L, Kunert KJ, Pruvost C, Polle A, Foyer HC, Rennenberg H (1995) Regulation of glutathione synthesis in leaves of transgenic poplar (*Populus tremula x P. alba*) overexpressing glutathione synthetase. Plant J 7:141–145.

Swartzberg D, Kirshner B, Rav-David D, Elad Y, Granot D (2008) *Botrytiscinereal* induces senescence and is inhibited by autoregulated expression of the IPT gene. Eur J Plant Pathol 120:289–297.

Tamura K, Stecher G, Peterson D, Filipski A, Kumar S (2013) MEGA6: molecular evolutionary genetics analysis version 6.0. Mol Biol Evol 30: 2725–2729.

Tanaka R, Kobayashi K, Masuda T (2011) Tetrapyrrole metabolism in *Arabidopsis thaliana*. Arabidopsis Book 9:e0145.

Terhonen E, Blumenstein K, Kovalchuk A, Asiegbu FO (2019) Forest tree microbiomes and associated fungal endophytes: functional roles and impact on forest health. Forests 10:42.

Ton J, Flors V, Mauch-Mani B (2009) The multifaceted role of ABA in disease resistance. Trends Plant Sci 14:310–317.

Torres MA (2010) ROS in biotic interactions. Physiol Plant 138:414–429.

Vadassery J, Reichelt M, Hause B, Gershenzon J, Boland W, Mithöfer A (2012) CML42-mediated calcium signaling coordinates responses to *Spodoptera* herbivory and abiotic stresses in *Arabidopsis*. Plant Physiol 159:1159–1175.

Van MA, Bihon W, Vos LD, Naidoo K, Roodt D, Van D et al. (2014) Draft genome sequences of *Diplodia sapinea*, *Ceratocystis manginecans*, and *Ceratocystis moniliformis*. IMA Fungus 5:135–140.

Van Soest PJ (1963) Use of detergents in the analysis of fibrous feeds. II. A rapid method for the determination of fibre and lignin. J Assoc Of Anal Chem 46:829–835.

Vanstraelen M, Benkova E (2012) Hormonal interactions in the regulation of plant development. Annu Rev Cell Dev Biol 28:463–487.

Velikova V, Yordanov I, Edreva A (2000) Oxidative stress and some antioxidant systems in acid rain-treated bean plants: protective role of exogenous polyamines. Plant Sci 151:59–66.

Vornam B, Leinemann L, Peters FS, Wolff A, Leha A, Salina G, Schumacher J, Gailing O (2019) Response of scots pine (*Pinus sylvestris*) seedlings subjected to artificial infection with the fungus *Sphaeropsis sapine*a. Plant Mol Biol Rep 37: 214–223.

Wallis C, Eyles A, Chorbadjian R, McSpadden GB, Hansen R, Cipollini D, Bonello P (2008) Systemic induction of phloem secondary metabolism and its relationship to resistance to a canker pathogen in Austrian pine. New Phytol 177:767–778.

Walters DR, McRoberts N (2006) Plants and biotrophs: a pivotal role for cytokinins? Trends Plant Sci 11:581–586.

White TJ, Bruns T, Lee S, Taylor J (1990) Amplification and direct sequencing of fungal ribosomal RNA genes for phylogenetics. In: Innis MA, Gelfand DH, Sninsky JJ, White TJ (eds) PCR protocols: a guide to methods and applications. Academic Press, New York, pp 315–322.

Xiao D, Cui Y, Xu F, Xu X, Gao G, Wang Y, Guo Z, Wang D, Wang NN (2015) SENESCENCE-SUPPRESSED PROTEIN PHOSPHATASE directly interacts with the cytoplasmic domain of SENESCENCE-ASSOCIATED RECEPTOR-LIKE KINASE and negatively regulates leaf senescence in *Arabidopsis*. Plant Physiol 169:1275–1291.

Xu YX, Xiao MZ, Liu Y, Fu JL, He Y, Jiang DA (2017) The small auxin-up RNA OsSAUR45 affects auxin synthesis and transport in rice. Plant Mol Biol 94:97–107.

Yu G, Wang LG, Han Y, He QY (2012) clusterProfiler: an R package for comparing biological themes among gene clusters. Omics 16:284–287.

Zhang SH, Yang Q, Ma RC (2007) *Erwinia carotovora* ssp. *carotovora* infection induced "defense lignin" accumulation and lignin biosynthetic gene expression in Chinese cabbage (*Brassica rapa* L. ssp. *pekinensis*). J Integr Plant Biol 49:993–1002.

Zhang Z, Schwartz S, Wagner L, Miller W (2000) A greedy algorithm for aligning DNA sequences. J Comput Biol 7:203–214.

Zhang ZH, Jhaveri DJ, Marshall VM et al. (2014) A comparative study of techniques for differential expression analysis on RNA-seq data. PLoS One 9:e103207. https://doi.org/10.1371/journal.pone.0103207.

Zheng XY, Spivey NW, Zeng W, Liu PP, Fu ZQ et al. (2012) Coronatine promotes pseudomonas syringae virulence in plants by activating a signaling cascade that inhibits salicylic acid accumulation. Cell Host Microbe 11:587–596.